NASA TN D-1477

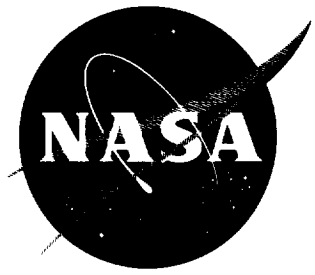


# TECHNICAL NOTE

D-1477

## A PRELIMINARY EXPERIMENTAL INVESTIGATION OF AN ENERGY-ABSORPTION PROCESS EMPLOYING FRANGIBLE METAL TUBING

By John R. McGehee

Langley Research Center
Langley Station, Hampton, Va.

NATIONAL AERONAUTICS AND SPACE ADMINISTRATION
WASHINGTON October 1962

NATIONAL AERONAUTICS AND SPACE ADMINISTRATION

TECHNICAL NOTE D-1477

# A PRELIMINARY EXPERIMENTAL INVESTIGATION OF AN ENERGY-ABSORPTION PROCESS EMPLOYING FRANGIBLE METAL TUBING

By John R. McGehee

## SUMMARY

A highly efficient energy-absorption process, employing frangible metal tubing as the working element, was investigated. A preliminary experimental investigation has been conducted to determine the variation of the average fragmenting stress of 2024-T3 aluminum-alloy tubing with the pertinent parameters of this process. Limited tests were made to determine the feasibility of employing this process in a landing-gear system. A 1/5-scale model of a proposed manned spacecraft with a landing gear incorporating this process was employed in these tests.

The results of this investigation show that the fragmenting process produces a fluctuating force with displacement, but for a fixed set of parameters, the force about which the fluctuation occurs is approximately constant. A large force which occurs when the process is started with the unaltered tube seated symmetrically in the die can be reduced most effectively by tapering the wall thickness over a short length at the die end of the tube. The average fragmenting stress, for 2024-T3 aluminum-alloy tubing and the range of parameters investigated, appears to be independent of the ratio of wall thickness to tube diameter, but varies as the cube of the ratio of the wall thickness to the radius of the forming die. The fragmenting stress obtained at 12,000 inches per minute was about 60 percent higher than those obtained at 1 inch per minute. The 2024-T3 aluminum-alloy tubing, when fragmenting on a die at 90 percent of the yield stress, is capable of absorbing 31,000 foot-pounds of energy per pound of material. This energy-absorption capability is greater than that of the most frequently considered processes; for example, the crushing of balsa wood, aluminum honeycomb, or pressurized thin-walled metallic cylinders. Model tests, employing frangible tubing as the working element in the landing gear, indicate that this process is suitable for use in a load-alleviation application.

## INTRODUCTION

The stringent volume, weight, and environmental requirements for spacecraft landing systems have resulted in an intensified research program on energy-absorption processes. A portion of this research effort has led to the development of a highly efficient energy-absorption process which employs frangible metal tubing as the working element.

Literature on the subject of energy absorption includes many processes. A list of some of the processes which have been employed in or proposed for landing-gear systems would include pressurized and unpressurized air bags (refs. 1 and 2), thin-wall metallic cylinders (ref. 3), yielding and bending metal elements (ref. 4), crushing of various materials (ref. 5), devices utilizing friction, and the controlled flow of fluids. Several processes that have been investigated are presented in reference 6.

The fragmenting process, presented in this paper, absorbs energy through the force developed when a frangible tube is pressed over a die. The die is shaped so that the portion of the tube in contact with the die is split into segments and the segments are broken into small fragments. A fluctuating force is developed by the fragmenting process, but the force about which the fluctuation occurs is approximately constant. The breaking and dispersing of the segments of the tube permit the entire length of the working element to be employed as the working stroke. An experimental investigation, employing 2024-T3 aluminum-alloy tubing, has been conducted to determine the variation of the fragmenting force with the pertinent parameters and to ascertain the feasibility of the use of this process in a load-alleviation application.

## SYMBOLS

| | |
|---|---|
| A | area of cross section of tubing, $\pi D_m t$, sq in. |
| a | acceleration, $ft/sec^2$ |
| C | fragmenting coefficient, $\sigma_f/(t/r)^3$, ksi |
| D | outside diameter of tubing, in. |
| F | axial force, lb |
| g | acceleration due to gravity, 32.2 $ft/sec^2$ |
| I | moment of inertia, $slug\text{-}ft^2$ |

| | |
|---|---|
| $l$ | length, in. |
| m | mass, slugs |
| r | forming radius of die, in. |
| t | average wall thickness of tubing, $\frac{\text{Weight of measured length}}{\rho \pi l \left(D - t_{\text{nominal}}\right)}$, in. |
| V | velocity, fps |
| X,Z | body axes (fig. 5) |
| $\alpha$ | angular acceleration, radians/sec$^2$ |
| $\delta$ | displacement, in. |
| $\dot{\delta}$ | rate of displacement, in./min |
| $\rho$ | density of aluminum alloy, lb/cu in. |
| $\sigma$ | stress, F/A, psi |
| $\tau$ | time, sec |
| $\omega$ | angular velocity, radians/sec |

Subscripts:

| | |
|---|---|
| f | average during fragmenting |
| m | mean |

## APPARATUS AND PROCEDURE

### Parametric Investigation

The present investigation is concerned with establishing the variation of the fragmenting force, developed from 2024-T3 aluminum-alloy tubing, with the pertinent parameters and with the limitations imposed upon the fragmenting process. The fragmenting regime, as defined for this investigation, is the range of parameters within which the segments were broken before the leading edges of the segments left the forming section of the die. To reduce the possibility of column buckling, the specimens were limited to length to diameter ratios of 10 or less (short column range).

A sketch illustrating the fragmenting process and the cross section of a typical die is shown in figure 1. The forming section of the dies is semicircular in cross section and circular in planform. The dies used in the investigation conducted at low rates of displacement were machined with a 1-inch-long cylindrical guide shaft which had a diameter approximately 0.004 inch smaller than the inside diameter of the tube for which it was designed. The end of the guide shaft was rounded to alleviate gouging of the tube in the event of misalinement during operation. The die used in the investigation conducted at high rates of displacement differed only in the length of the guide shaft. The transition between the shaft and the forming section of the die was smooth. Some of the dies were machined from tool steel and heattreated to a Rockwell hardness number of C-38. Other dies were machined from cold-rolled steel and after being used with as many as six specimens, no discernible change in the shape of the forming section could be detected by using radius gages.

The investigation at low rates of displacement was conducted in a 100,000-pound-capacity universal static hydraulic testing machine at the Langley Research Center. A sketch of the test setup is shown in figure 2. The outputs from strain gages on a thin cantilever beam, activated by the weighing system of the testing machine and from a linear potentiometer were recorded on an oscillograph. The frequency response of the galvanometers, used for recording forces and displacements, is flat to about 200 cycles per second.

The brief investigation at high rates of displacement was conducted on the 10,000-pound-capacity high-speed pneumatic tensile testing machine at the Langley Research Center. This testing machine and its operation are described in reference 7. A sketch of the test setup is shown in figure 3. An adapter was attached to the base of the machine to accommodate the application of compressive forces required for this investigation. The force was measured by a 10,000-pound-capacity load cell, and the displacement was measured by a linear potentiometer. The outputs from the load cell and the linear potentiometer were recorded on an oscillograph at a paper speed of 500 inches per second. The galvanometers, used for recording forces and displacements, have a frequency response flat to about 1,300 cycles per second.

The present tests were conducted on 2024-T3 aluminum-alloy tubing for a range of outside diameters from 0.25 inch to 2.0 inches and a range of wall thicknesses from 0.020 inch to 0.065 inch. The average tube-wall thickness was determined by weighing known lengths of the tubing of the various diameters and computing the thicknesses. The computed thickness is used in determining stress, $t/r$, and $t/D$. The tests for the high rates of displacement were conducted by using only 1-inch-diameter, 0.065-inch wall thickness tubing. The tubes were cut to the desired length, and the ends were squared by turning the tubes on a lathe. The working face of the die was coated with light oil and

sprinkled with molybdenum disulphide powder in order to reduce friction. The low rate of displacement was approximately 1 inch per minute, and the range of high rates of displacement investigated was 9,600 to 12,600 inches per minute.

When the tube is seated symmetrically in the die, a large force is required to start the fragmenting process. Therefore, to obtain fragmenting forces approaching the yield strength of the tubing material it was necessary to reduce the large initial peak force in order to prevent column failure. Two methods for reducing this peak force were investigated. One method consisted of initially fragmenting the tube over a die with a forming radius larger than the forming radius of the operating die. Then the tube, with the fragmented end, was installed on the operating die, and larger average values of the fragmenting force could be obtained without column buckling. The second method consisted of machining an external taper on the wall thickness of the die end of the tube permitting fragmenting to be initiated at considerably reduced forces. This method also permits some control of the rate of onset of the fragmenting force through regulation of the length of the tapered portion of the tube-wall thickness.

## Model Investigation

A 1/5-scale model of a proposed manned spacecraft was landed from a vertical flight path at a $0^{\circ}$ contact attitude for a contact velocity corresponding to 30 fps full scale. The model was also landed from an oblique flight path (approximately $35^{\circ}$) at a contact attitude of $12^{\circ}$ for a vertical contact velocity corresponding to 13.5 fps full scale and a horizontal contact velocity corresponding to 18 fps full scale. Scaling was as shown in table I.

A photograph of the model used in landing from a vertical flight path is shown in figure 4. The upper part of the model consisted of a lead disk with a plastic conical section. A plywood disk was used to simulate the heat shield. The landing gear consisted of four dies and four 2024-T3 aluminum-alloy tubes 7 inches long with 0.75-inch outside diameter and 0.065-inch wall thickness attached between the model and the simulated heat shield. The tubes and dies were oriented vertically and located symmetrically about the center of the planform of the model, approximately on the circumference of the radius of gyration. The model weighed 1,120 pounds, had a maximum diameter of 28 inches, and was 12 inches high. (See table II.)

These tests were made by a free-fall method where the model was dropped from the height required to obtain (under the influence of gravitational acceleration) a vertical velocity of 13.42 feet per second at contact. Normal accelerations were measured by strain-gage accelerometers, rigidly attached at the center of gravity of the model, and were

recorded on an oscillograph. The accelerometers were capable of measuring accelerations of 50g and 25g along the X-axis. (See fig. 4.) The 50g accelerometer has a natural frequency approximately double that of the 25g accelerometer. Therefore, to determine if there was an effect of frequency response on the average fragmenting load, both accelerometers were mounted to measure accelerations along the X-axis. The natural frequency of the 50g accelerometer was about 630 cycles per second and that of the 25g accelerometer was about 350 cycles per second. The accelerometers were damped to about 65 percent of critical damping. The response of the recording equipment was flat to about 135 cycles per second. Motion pictures were taken to study the action of the tubes as they fragmented.

The frangible tubes have very little resistance to shear forces as they are operating on the dies; therefore, the force applied to the tube-die combination must act approximately parallel to the long axis of the tube. For landings from oblique flight paths it is necessary to use a linkage system (or some similar system) to insure that forces are transmitted to the tube-die combinations along the long axis of the tubes. The linkage system used consisted of two steel tube X-frames mounted in tandem between the simulated heat shield and the body of the model. See figures 5(a) and 5(b). The simulated heat shield was a segment of a sphere and was constructed of fiber glass and plastic. This shape was employed to insure a smooth rocking action and force application for landing attitudes other than $0^{\circ}$. The dies and restraining plates were pivoted in the fore and aft directions to permit force application parallel to the long axis of the tubes as the simulated heat shield shifted relative to the body during impact. The energy-absorption system consisted of two dies and two 2024-T3 aluminum-alloy tubes 7 inches long with a 1-inch outside diameter and a 0.065-inch wall thickness. The dies had guide shafts 1 inch long and diameters 0.004 inch smaller than the inside diameter of the tubes. The bucking plates were drilled to allow the shafts of the dies to pass and were counterbored to restrain the upper end of the tubes. The design permitted maximum utilization of the working material (full stroke). The tubes and dies were attached to the simulated heat shield and the model at points, determined from design calculations, which would minimize rotational motions and maintain forces in the linkage system within operating limits.

The landings were made by using a pendulum arrangement to obtain a flight-path angle of approximately $36^{\circ}$ and a contact attitude of $12^{\circ}$. This test procedure is discussed in detail in reference 8. Accelerations along the X- and Z-axes (see fig. 5(a)) were measured and recorded by the instrumentation discussed previously. The 50g accelerometer was alined along the X-axis and the 25g accelerometer was alined along the Z-axis. Motion pictures were taken to study the action of the landing-gear system.

# RESULTS AND DISCUSSION

## Parametric Investigation

Low rate of displacement.- Typical variations of the axial force developed during fragmentation are shown in figure 6 as a function of the displacement of the tube over the die at a rate of displacement of 1 inch per minute. The data presented in this figure were obtained from tests of 2024-T3 aluminum-alloy tubes having 1-inch outside diameter and 0.065-inch wall thickness. The tubes had squared ends and full wall thickness and were fragmented over a die having a ratio of tube wall thickness to die forming radius $t/r$ of 0.40. The large initial peak force is required to start the fragmenting process when the specimen has squared ends and full wall thickness and is seated symmetrically in the die. The large difference in the magnitude of the initial peak force and the peak forces which occur after the process has been started may be attributed primarily to the force required to initiate the circumferential expansion and subsequent splitting of the tube. Methods investigated for reducing this initial peak force will be discussed in the following paragraph. After the process has started, the tube continues to split into segments, and the segments are formed in the die and break into fragments. This procedure results in the production of fluctuating forces, but the average value of these fluctuating forces is approximately constant and is shown on the figure as the average fragmenting force.

The relative effectiveness of the two methods investigated for reducing the large initial peak force is shown by the faired force-displacement curves of figure 7. These tests were conducted using 2024-T3 aluminum-alloy tubing of 0.5-inch outside diameter and 0.065-inch wall thickness. The $t/r$ for these tests was 0.43, and the rate of displacement was approximately 1 inch per minute. The radius of the forming section of the die was selected so that the initial starting force would not exceed the column strength. The solid curve is the faired force-displacement curve obtained from a squared-end specimen with full wall thickness. As shown in the figure, the initial peak force for this specimen was approximately 300 percent of the average fragmenting force. The dashed curve is the faired force-displacement curve obtained from a specimen which had been fragmented on the die over a displacement of approximately 0.5 inch prior to the tests. The initial peak force in this case was only 150 percent of the average fragmenting force. The dash-dot curve is the faired force-displacement curve obtained from a squared-end specimen with a tapered wall thickness extending approximately 0.5 inch along the length of the tube at the die end of the specimen. The initial peak force in this case was approximately the same as the average fragmenting force.

The average axial force during fragmentation (average fragmenting force) produced by the unaltered specimen was approximately 120 percent of the average fragmenting force produced by either of the altered specimens. This difference may be attributed to the variation in temper of the material of the specimens, variation in frictional force produced during the tests, experimental accuracy, or a combination of these factors. The major effect of tube-end condition is on the initial peak force and there is little or no effect on the average fragmenting force.

The fragmenting stress $\sigma_f$ (average axial force during fragmenting divided by the cross-sectional area of the tube) is shown in figure 8 as a function of tube wall thickness-diameter ratio $t/D$ for a ratio of tube wall thickness to die forming radius $t/r$ of 0.43. The data are for tubes having a wall thickness of 0.065 inch and the range of tube diameters investigated. The fairing of the data indicate that the fragmenting stress is independent of $t/D$.

The fragmenting stress is shown as a function of $t/r$ in figure 9 with nominal wall thickness as a parameter. The data are plotted on logarithmic scales for the range of outside diameters and wall thicknesses investigated. The solid line is a fairing of the data obtained from tests of tubes with wall thicknesses of 0.065 inch. The fairing of the data indicates that the fragmenting stress varies as $(t/r)^3$.

The end points of the range of $t/r$ for fragmentation were not accurately established in this investigation. The tabulated data (table III) generally show that at $t/r$ values of 0.67 column failure occurred and for the smaller wall thicknesses, at $t/r$ values less than approximately 0.30, rolling or a combination of rolling and breaking occurred. When rolling or rolling and breaking occurred it would be expected that the stress would not vary as the cube of $t/r$. The variation of stress with $t/r$ for the rolling or rolling and breaking regimes was not determined in this investigation.

The data points obtained from tests of tubes with wall thicknesses less than 0.065 inch indicate column stresses during fragmenting generally higher than those indicated by the cube of the parameter $t/r$. These higher stresses may be due to inaccuracies in the radii of the forming sections of the dies, to greater physical properties of the material in the thinner wall tubing, or to a thickness variation which was introduced by the inclusion of wall thickness in the computation of the stress.

Data in figure 9 are replotted in figure 10 with experimental fragmenting stress as a function of $(t/r)^3$ with nominal wall thickness as a parameter. The fragmenting coefficient $C$ determined as the slope of the fairing of the data for a wall thickness of 0.065 inch is 171 ksi. Hence the fragmenting stress, for 2024-T3 aluminum-alloy tubing within

the range of parameters investigated, may be obtained from the following tentative equation:

$$\sigma_f = 171(t/r)^3$$

High rates of displacement.- Typical fragmenting-force variations are shown in figure 11 as a function of the displacement of the tube over the die for a rate of displacement of 9,600 inches per minute. Aluminum-alloy tubing (2024-T3) of 1-inch diameter and 0.065-inch wall thickness was used in these tests. As was the case for the tests conducted at a rate of displacement of 1 inch per minute, the tapered wall thickness at the die end of the specimen was very effective in reducing the initial peak force. The fragmenting tube produced a fluctuating force but the average force about which the fluctuations occurred was approximately constant and was substantially greater than that for the same tubing tested at a rate of displacement of 1 inch per minute.

The variation of the fragmenting stress with rate of displacement is shown in figure 12. Data presented in reference 9 indicate no significant increase in tensile yield or tensile ultimate strength of aluminum alloys for rates of displacement below approximately 5,000 inches per minute. Therefore, the fairing of the data presented in this figure was made with the assumption that there was no change in fragmenting stress below a rate of displacement of 5,000 inches per minute. The data shown at a rate of displacement of 1 inch per minute were obtained from the same die that was used at the high rates of displacement in order to alleviate the effects of possible errors in die radius. At a rate of displacement of 12,000 inches per minute, the fragmenting stress is approximately 160 percent of the fragmenting stress obtained at a rate of displacement of 1 inch per minute.

Energy absorption capabilities.- The energy absorption capabilities of various materials and processes are presented in bar-graph form in figure 13. The data for the pressurized metallic cylinder are from reference 3, and for aluminum honeycomb and balsa wood from reference 5. The values of energy absorbed per pound of working material from references 3 and 5 were determined from the average collapsing force obtained from dynamic tests. The energy absorbed per pound of material for the fragmenting tube was determined from the average fragmenting force obtained from tests conducted at a rate of displacement of 1 inch per minute. The 2024-T3 aluminum-alloy tubing, when fragmenting on a die at a value of fragmenting stress equal to a value of 90 percent of the yield stress of the material, is capable of absorbing 31,000 foot-pounds of energy per pound of material. As shown in figure 13 this value is greater than that of the high-energy dissipation capability of balsa wood crushed parallel to the grain. It is also of interest to note that the balsa wood crushed

parallel to the grain may have violent rebound characteristics, depending upon the design, and that the working stroke is limited to about 80 percent of the initial length because of bottoming. The fragmenting tube has negligible rebound and the full length of the tube may be used to provide the decelerating force.

## Model Investigation

Landings from vertical flight path.- A typical time history of accelerations along the X-axis for the model landing from a vertical flight path at a $0^{\circ}$ contact attitude is shown in figure 14 for a contact velocity of 13.5 fps (30 fps full scale). The initial peak acceleration results from the large force required to start fragmenting the tubes when they have full wall thickness, squared ends, and rest symmetrically in the dies. This initial peak acceleration could have been reduced considerably if the die ends of the tubes had been prefragmented or if the wall thickness had been tapered prior to the drop test. After the fragmenting process has started, the acceleration is approximately constant, as indicated by the dashed line. The peak acceleration which results at the end of the acceleration time history may possibly be attributed to a force which corresponds to the force necessary to start fragmenting a prefragmented tube from rest. It does not appear unreasonable to compare the action of the tubes at the end of the decelerating period of the model test - rate of displacement approaching zero - with that of the starting of a prefragmented tube from rest. The initial peak force for a tube with the die end prefragmented was about 50 percent greater than the average fragmenting force (figs. 6 and 7). The peak values of acceleration measured by both the 50g and 25g accelerometers were approximately 10.5g and the average value of acceleration for the major portion of the decelerating period was approximately 6.5g. Sequence photographs of the model landing from a vertical flight at a $0^{\circ}$ contact attitude are shown in figure 15.

Landings from oblique flight path.- A typical time history of accelerations along the X-axis for the model landing on concrete from a $33^{\circ}$ flight path at a contact attitude of approximately $11^{\circ}$ is shown in figure 16. The vertical velocity at contact was 4.7 fps (10.5 fps full scale) and a horizontal velocity of 7.3 fps (16.3 fps full scale). The die ends of the two tubes were prefragmented prior to installation to reduce the initial peak force. The initial peak acceleration was about 3g, and the peak occurring at the end of the accelerating period was about 5g. A constant acceleration of about 2.2g was maintained over the major portion of the decelerating period. The peak which occurred near the middle of the acceleration time history resulted from the impact of the trailing edge of the body as the body rocked on the spherical heat shield. This impact could possibly be eliminated by a more precise design. The peak Z-axis accelerations were less than 2g, and the constant

Z-axis acceleration was less than 1g. Sequence photographs of the model landing from an oblique flight path are shown in figure 17.

The model tests demonstrate the use of the fragmenting-tube process in a load-alleviation application. The average fragmenting force, computed from the acceleration time histories for a single tube, was approximately the same as that predicted by the tests conducted at a rate of displacement of 1 inch per minute. The rate of displacement varied from a high value of 9,700 inches per minute to zero during a dynamic model test. As shown in figure 12, the fragmenting stress, and consequently the fragmenting force, increased with increasing rate of displacement. The acceleration time histories from the model tests should have shown the effect of the initial high rate of displacement through a gradually decreasing acceleration in the early portion of the acceleration time history, but this was not detected.

## CONCLUDING REMARKS

The results of the preliminary experimental investigation of the frangible-tube energy-dissipation process show that the fragmenting tubes produce a fluctuating force with displacement; but for a fixed set of parameters, the average value of the force about which this fluctuation occurs is approximately constant. The large force, which occurs when the process is started with the unaltered tube seated symmetrically in the die, can be reduced most effectively by tapering the wall thickness over a short length at the die end of the tube. The average fragmenting stress, for 2024-T3 aluminum-alloy tubing and the range of parameters investigated, appears to be independent of the ratio of wall thickness to tube diameter, but generally varies as the cube of the ratio of wall-thickness to the radius of the forming section of the die. The fragmenting stress obtained at a rate of displacement of 12,000 inches per minute was 160 percent of that obtained at 1 inch per minute. The 2024-T3 aluminum-alloy tubing, when fragmenting on a die with a fragmenting stress equal to 90 percent of the material yield stress, is capable of absorbing 31,000 foot-pounds of energy per pound of material. This energy-absorption capability is greater than that of the most frequently considered processes; for example, the crushing of balsa wood, aluminum honeycomb, or pressurized thin-walled metallic cylinders. Model tests, employing 2024-T3 aluminum-alloy tubing as the working element in the landing gear, indicate that the process is suitable for use in a load-alleviation application.

Langley Research Center,
National Aeronautics and Space Administration,
Langley Station, Hampton, Va., July 11, 1962.

## REFERENCES


1. McGehee, John R., and Hathaway, Melvin E.: Landing Characteristics of a Reentry Capsule With a Torus-Shaped Air Bag for Load Alleviation. NASA TN D-628, 1960.

2. McGehee, John R., and Vaughan, Victor L., Jr.: Model Investigation of the Landing Characteristics of a Reentry Spacecraft With a Vertical-Cylinder Air Bag for Load Alleviation. NASA TN D-1027, 1962.

3. Coppa, Anthony P.: Collapsible Shell Structures for Lunar Landings. [Preprint] 2156-61, American Rocket Soc., Oct. 1961.

4. Hoffman, Edward L., Stubbs, Sandy M., and McGehee, John R.: Effect of a Load-Alleviating Structure on the Landing Behavior of a Reentry-Capsule Model. NASA TN D-811, 1961.

5. Brooks, G. W., and Carden, Huey D.: A Versatile Drop Test Procedure for the Simulation of Impact Environments. Noise Control Shock and Vibration, vol. 7, no. 5, Sept.-Oct. 1961, pp. 4-8.

6. Fisher, Lloyd J., Jr.: Landing-Impact-Dissipation Systems. NASA TN D-975, 1961.

7. Heimerl, G. J., and Manning, C. R., Jr.: A High-Speed Pneumatic Tension Testing Machine. Materials Res. and Standards, vol. 2, No. 4, April 1962, pp. 270-275.

8. McGehee, John R., Hathaway, Melvin E., and Vaughan, Victor L., Jr.: Water-Landing Characteristics of a Reentry Capsule. NASA MEMO 5-23-59L, 1959.

9. Kaufman, J. G.: Summary Report - The Effects of High Strain Rates on The Mechanical Properties of Aluminum Alloys. Rep. No. 9-60-31, ALCOA Res. Labs., Aluminum Co. of America, Aug. 15, 1960.

TABLE I.- SCALING FACTORS*

[Scale factor $\lambda = 1/5$]

| | Full scale | Scale factor | Model scale |
|---|---|---|---|
| Acceleration . . . . . | a | 1 | a |
| Stress . . . . . | $\sigma$ | 1 | $\sigma$ |
| Length . . . . . | $l$ | $\lambda$ | $\lambda l$ |
| Time . . . . . | $\tau$ | $\sqrt{\lambda}$ | $\sqrt{\lambda}\ \tau$ |
| Velocity . . . . . | V | $\sqrt{\lambda}$ | $\sqrt{\lambda}$ V |
| Angular velocity . . . . . | $\omega$ | $1/\sqrt{\lambda}$ | $\omega/\sqrt{\lambda}$ |
| Angular acceleration . . . | $\alpha$ | $1/\lambda$ | $\alpha/\lambda$ |
| Mass . . . . . | m | $\lambda^2$ | $K\lambda^2 M$ |
| Force . . . . . | F | $\lambda^2$ | $K\lambda^2 F$ |
| Density . . . . . | $\rho$ | $1/\lambda$ | $\rho/\lambda$ |
| Moment of inertia . . . . | I | $\lambda^4$ | $\lambda^4 I$ |

*To insure landing stability for the model used in landings from a vertical flight path, four tubes of 0.75-inch diameter and 0.065-inch wall thickness were used. The force obtained from one of these tubes would have been adequate to accomplish the desired deceleration. Therefore, the scaled mass and scaled force were both increased by the factor $K = 4$ inasmuch as the only requirement for maintaining identical accelerations for model and full scale is that the force-mass ratio must remain the same for the model and the full-scale configurations. The model used in landings from an oblique flight path employed two tubes of 1-inch diameter and 0.065-inch wall thickness to give the same scaled mass and force relationship.

TABLE II.- PERTINENT DIMENSIONS OF 1/5-SCALE MODEL

AND FULL-SCALE SPACECRAFT

| | 1/5 scale | Full scale |
|---|---|---|
| Maximum diameter of configuration, ft . . . | 2.33 | 11.7 |
| Height of configuration, ft . . . . . | 1 | 5.0 |
| Weight of configuration, lb . . . . . | 1,120 | 7,000 |
| Location of center of gravity from top of configuration, ft . . . . . | 0.74 | 3.7 |

TABLE III.- DATA IN TABULAR FORM

| t, in. | D, in. | R, in. | $\dot{\delta}$, in./min | Average force, lb | $\sigma_f$, ksi | t/D | t/r | Operating regime |
|---|---|---|---|---|---|---|---|---|
| 0.020 | 0.25 | 0.062 | 1 | 450 | 31.0 | 0.080 | 0.32 | Rolling and breaking |
| .020 | .25 | .062 | 1 | 470 | 32.4 | .080 | .32 | Rolling and breaking |
| .020 | .25 | .062 | 1 | 460 | 31.7 | .080 | .32 | Rolling and breaking |
| .020 | .414 | .125 | 1 | 240 | 9.7 | .048 | .16 | Rolling |
| .020 | .665 | .042 | 1 | 1,500 | 37.0 | .030 | .476 | Fragmentation |
| .020 | .664 | .042 | 1 | 1,350 | 33.3 | .030 | .476 | Fragmentation |
| .020 | .665 | .042 | 1 | 1,400 | 34.6 | .030 | .476 | Fragmentation |
| .021 | .414 | .125 | 1 | 255 | 9.8 | .051 | .17 | Rolling |
| .022 | .25 | .040 | 1 | 600 | 38.0 | .088 | .55 | Column buckled |
| .022 | .25 | .040 | 1 | 500 | 31.6 | .088 | .55 | Fragmentation |
| .022 | .25 | .047 | 1 | 430 | 27.2 | .088 | .47 | Fragmentation |
| .022 | .414 | .125 | 1 | 230 | 8.5 | .053 | .18 | Rolling |
| .022 | .25 | .047 | 1 | 450 | 28.5 | .088 | .47 | Fragmentation |
| .022 | .25 | .047 | 1 | 450 | 28.5 | .088 | .47 | Fragmentation |
| .022 | .25 | .040 | 1 | 570 | 36.1 | .088 | .55 | Fragmentation |
| .022 | .25 | .040 | 1 | 530 | 33.5 | .088 | .55 | Fragmentation |
| .022 | .25 | .040 | 1 | 560 | 35.4 | .088 | .55 | Fragmentation |
| .022 | .25 | .047 | 1 | 440 | 27.8 | .088 | .468 | Fragmentation |
| .022 | .25 | .047 | 1 | 440 | 27.8 | .088 | .468 | Fragmentation |
| .022 | .25 | .047 | 1 | 400 | 25.3 | .088 | .468 | Fragmentation |
| .028 | .50 | .062 | 1 | 1,050 | 25.3 | .056 | .45 | Rolling and breaking |
| .028 | .50 | .062 | 1 | 900 | 21.7 | .056 | .45 | Rolling and breaking |
| .028 | .50 | .062 | 1 | 900 | 21.7 | .056 | .45 | Rolling and breaking |
| .029 | .50 | .047 | 1 | Column buckled | | ----- | ----- | |
| .029 | .50 | .047 | 1 | Column buckled | | ----- | ----- | |
| .029 | .50 | .078 | 1 | 700 | 16.3 | .058 | .372 | Fragmentation |
| .029 | .50 | .078 | 1 | 800 | 18.6 | .058 | .372 | Fragmentation |
| .029 | .50 | .078 | 1 | 700 | 16.3 | .058 | .372 | Fragmentation |
| .029 | .500 | .052 | 1 | 1,350 | 31.5 | .058 | .558 | Fragmentation |
| .029 | .500 | .052 | 1 | 1,200 | 30.0 | .058 | .558 | Fragmentation |
| .029 | .500 | .052 | 1 | 1,280 | 29.8 | .058 | .558 | Fragmentation |
| .033 | .6895 | .109 | 1 | 1,080 | 15.9 | .048 | .30 | Rolling and breaking |
| .033 | .6900 | .109 | 1 | 1,080 | 15.7 | .048 | .30 | Rolling and breaking |
| .035 | .444 | .125 | 1 | 620 | 13.8 | .079 | .28 | Rolling and breaking |
| .0355 | .444 | .125 | 1 | 620 | 13.6 | .080 | .28 | Rolling and breaking |
| .0365 | .444 | .125 | 1 | 570 | 12.2 | .082 | .29 | Rolling and breaking |
| .044 | .710 | .109 | 1 | 1,800 | 19.5 | .062 | .404 | Fragmentation |
| .044 | .709 | .109 | 1 | 1,700 | 18.5 | .062 | .404 | Fragmentation |
| .044 | .710 | .109 | 1 | 1,750 | 19.0 | .062 | .404 | Fragmentation |
| .047 | .453 | .109 | 1 | 1,100 | 16.5 | .104 | .43 | Fragmentation |
| .047 | .453 | .109 | 1 | 1,000 | 15.0 | .104 | .43 | Fragmentation |
| .047 | .453 | .109 | 1 | 1,000 | 15.0 | .104 | .43 | Fragmentation |
| .047 | .453 | .109 | 1 | 950 | 14.2 | .104 | .43 | Fragmentation |
| .051 | .7295 | .109 | 1 | 2,500 | 24.5 | .070 | .468 | Fragmentation |
| .051 | .7290 | .109 | 1 | 2,450 | 24.0 | .070 | .468 | Fragmentation |
| .051 | .7300 | .109 | 1 | 2,600 | 25.5 | .070 | .468 | Fragmentation |
| .053 | .474 | .125 | 1 | 750 | 10.7 | .112 | .424 | Fragmentation |
| .053 | .474 | .125 | 1 | 800 | 11.4 | .112 | .424 | Fragmentation |
| .053 | .474 | .125 | 1 | 800 | 11.4 | .112 | .424 | Fragmentation |
| .063 | .500 | .150 | 1 | 1,200 | 13.9 | .126 | .420 | Fragmentation |
| .063 | .500 | .150 | 1 | 1,050 | 12.2 | .126 | .420 | Fragmentation |
| .063 | .500 | .150 | 1 | 1,100 | 12.7 | .126 | .420 | Fragmentation |

TABLE III.- DATA IN TABULAR FORM - Concluded

| t, in. | D, in. | R, in. | $\dot{\delta}$, in./min | Average force, lb | $\sigma_f$, ksi | t/D | t/r | Operating regime |
|---|---|---|---|---|---|---|---|---|
| 0.063 | 0.500 | 0.150 | 1 | 870 | 10.1 | 0.126 | 0.420 | Fragmentation |
| .063 | .500 | .150 | 1 | 1,050 | 12.2 | .126 | .420 | Fragmentation |
| .063 | .500 | .150 | 1 | 1,050 | 12.2 | .126 | .420 | Fragmentation |
| .065 | 1.0 | .163 | 1 | 2,100 | 11.0 | .065 | .4 | Fragmentation |
| .065 | 1.0 | .163 | 1 | 2,200 | 11.5 | .065 | .4 | Fragmentation |
| .065 | 1.0 | .163 | 1 | 2,000 | 10.5 | .065 | .4 | Fragmentation |
| .065 | 1.0 | .130 | 1 | 4,000 | 21.0 | .065 | .5 | Fragmentation |
| .065 | 1.0 | .130 | 1 | 3,800 | 19.9 | .065 | .5 | Fragmentation |
| .065 | 1.0 | .130 | 1 | 3,500 | 18.3 | .065 | .5 | Fragmentation |
| .065 | 1.0 | .098 | 1 | Column buckled | | ----- | .67 | |
| .065 | 1.0 | .098 | 1 | Column buckled | | ----- | .67 | |
| .065 | 1.0 | .098 | 1 | Column buckled | | ----- | .67 | |
| .065 | 1.0 | .098 | 1 | Column buckled | | ----- | .67 | |
| .065 | 1.0 | .098 | 1 | Column buckled | | ----- | .67 | |
| .065 | 1.0 | .130 | 1 | 3,300 | 17.3 | .065 | .5 | Fragmentation |
| .065 | 1.0 | .130 | 1 | 3,300 | 17.3 | .065 | .5 | Fragmentation |
| .065 | 1.0 | .130 | 1 | 3,500 | 18.3 | .065 | .5 | Fragmentation |
| .065 | 1.0 | .109 | 1 | 7,200 | 37.7 | .065 | .6 | Fragmentation |
| .065 | 1.0 | .109 | 1 | 7,000 | 36.6 | .065 | .6 | Fragmentation |
| .065 | 1.0 | .109 | 1 | 7,200 | 37.7 | .065 | .6 | Fragmentation |
| .065 | 1.0 | .109 | 1 | 7,000 | 36.6 | .065 | .6 | Fragmentation |
| .065 | .5 | .125 | 1 | Column buckled | | ----- | ----- | |
| .065 | .5 | .125 | 1 | Column buckled | | ----- | ----- | |
| .065 | .5 | .125 | 1 | 1,500 | 16.9 | .130 | .52 | Fragmentation |
| .065 | .5 | .150 | 1 | 1,000 | 11.3 | .130 | .43 | Fragmentation |
| .065 | .5 | .150 | 1 | 970 | 10.9 | .130 | .43 | Fragmentation |
| .065 | .5 | .125 | 1 | 1,450 | 16.8 | .130 | .504 | Fragmentation |
| .065 | .5 | .125 | 1 | 1,350 | 15.6 | .130 | .504 | Fragmentation |
| .065 | .5 | .125 | 1 | 1,300 | 15.0 | .130 | .504 | Fragmentation |
| .065 | .5 | .188 | 1 | 950 | 11.0 | .130 | .335 | Fragmentation |
| .065 | .75 | .150 | 1 | 1,750 | 12.5 | .087 | .43 | Fragmentation |
| .065 | .75 | .150 | 1 | 1,800 | 12.9 | .087 | .43 | Fragmentation |
| .065 | .75 | .150 | 1 | 1,700 | 12.2 | .087 | .43 | Fragmentation |
| .065 | .7535 | .109 | 1 | 4,800 | 34.1 | .086 | .60 | Fragmentation |
| .065 | 2.0 | .150 | 1 | 4,800 | 12.1 | .033 | .43 | Fragmentation |
| .065 | 2.0 | .150 | 1 | 4,800 | 12.1 | .033 | .43 | Fragmentation |
| .065 | 2.0 | .150 | 1 | 5,000 | 12.7 | .033 | .43 | Fragmentation |
| .065 | 1.0 | .150 | 1 | 2,400 | 12.6 | .065 | .43 | Fragmentation |
| .065 | 1.0 | .150 | 1 | 2,300 | 12.0 | .065 | .43 | Fragmentation |
| .065 | 1.0 | .150 | 1 | 2,300 | 12.0 | .065 | .43 | Fragmentation |
| .065 | 1.0 | .150 | 1 | 2,200 | 11.5 | .065 | .43 | Fragmentation |
| .065 | 1.0 | .150 | 1 | 2,300 | 12.0 | .065 | .43 | Fragmentation |
| .065 | 1.0 | .150 | 1 | 2,300 | 12.0 | .065 | .43 | Fragmentation |
| .065 | 1.0 | .150 | 1 | 2,300 | 12.0 | .065 | .43 | Fragmentation |
| .065 | 1.0 | .150 | 9,600 | 3,100 | 16.2 | .065 | .43 | Fragmentation |
| .065 | 1.0 | .150 | 9,600 | 3,300 | 17.3 | .065 | .43 | Fragmentation |
| .065 | 1.0 | .150 | 10,200 | 3,250 | 17.0 | .065 | .43 | Fragmentation |
| .065 | 1.0 | .150 | 12,000 | 3,350 | 17.5 | .065 | .43 | Fragmentation |
| .065 | 1.0 | .150 | 12,000 | 3,900 | 20.4 | .065 | .43 | Fragmentation |
| .065 | 1.0 | .150 | 12,600 | 4,000 | 20.9 | .065 | .43 | Fragmentation |

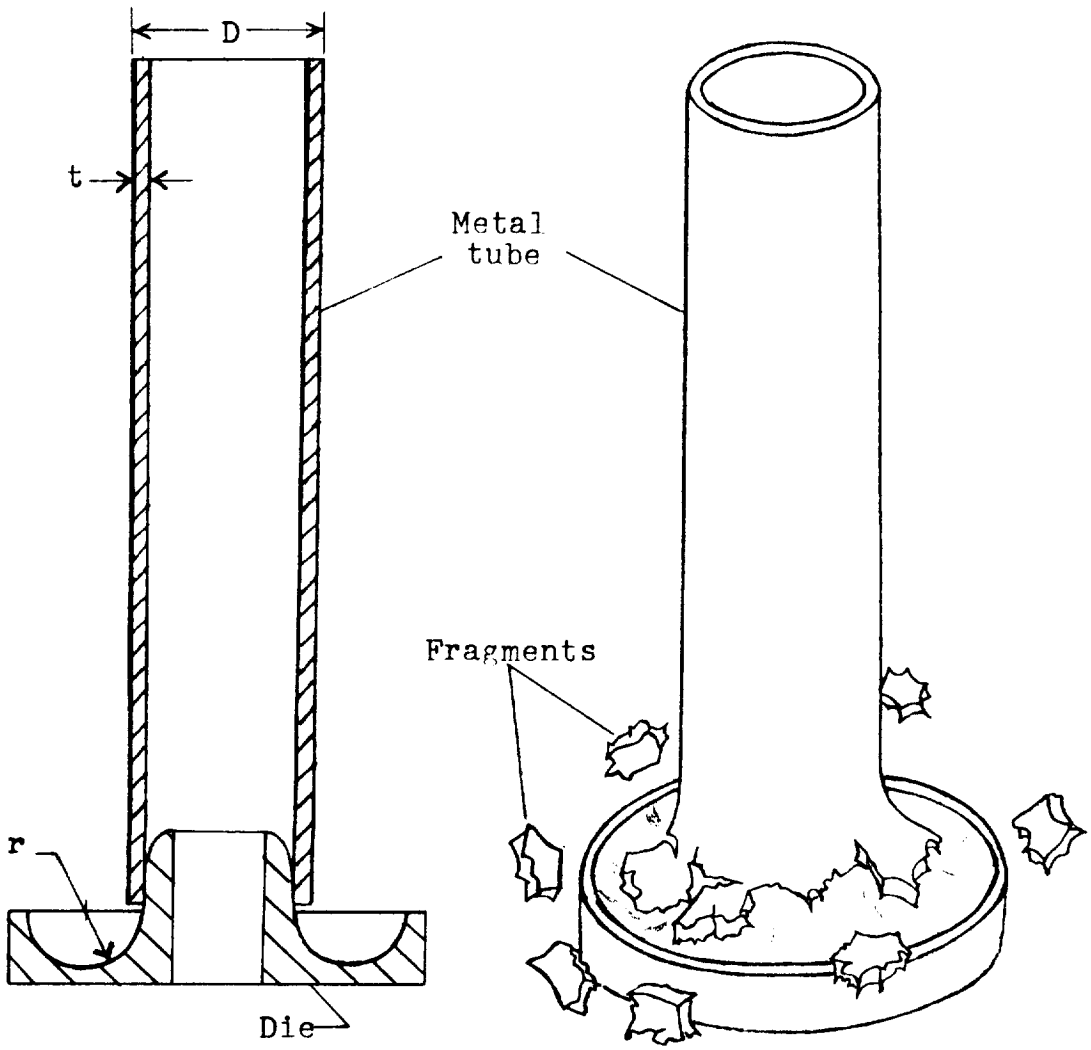


Figure 1.- Sketch illustrating fragmenting process.

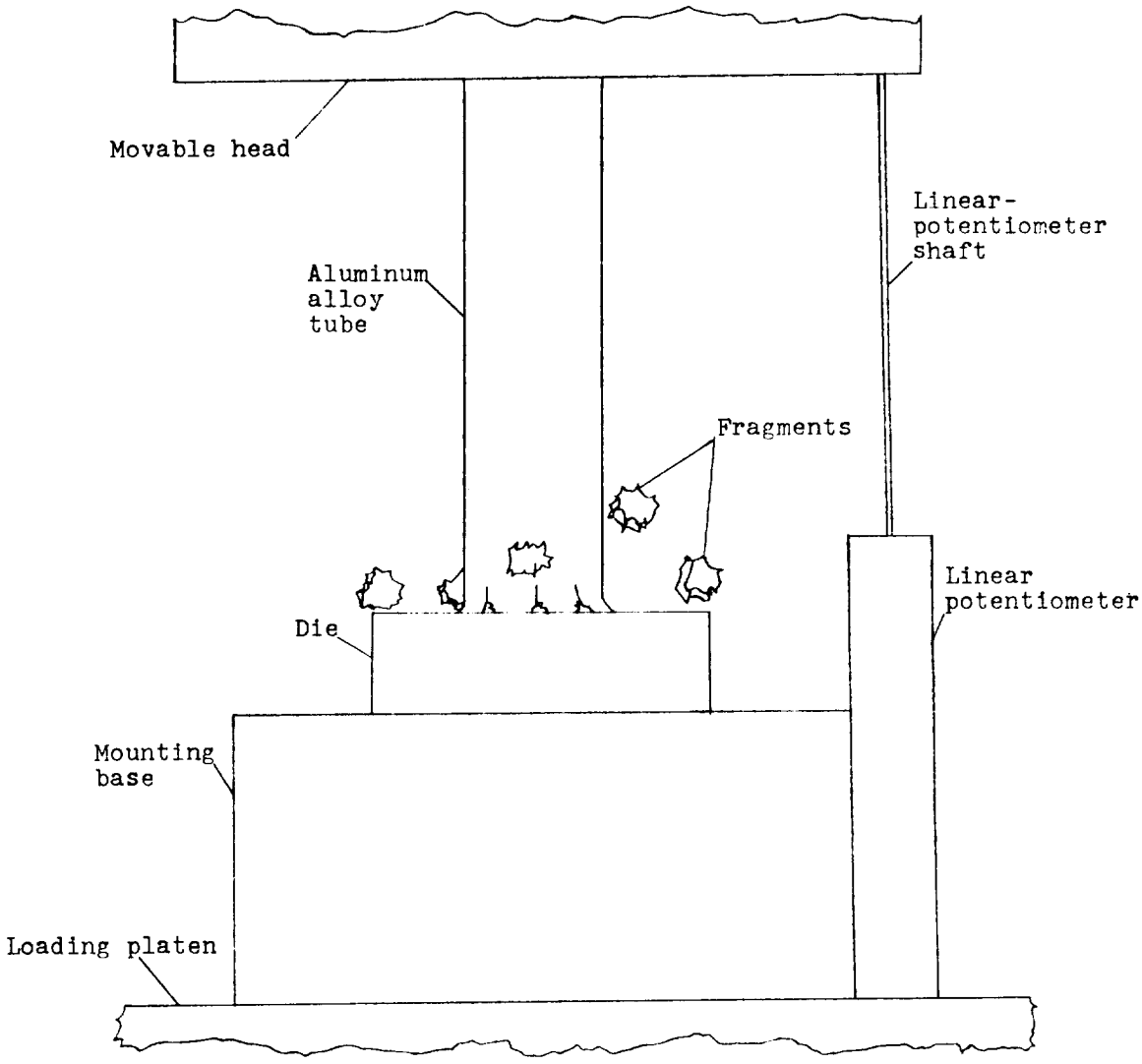


Figure 2.- Sketch of test setup for low-displacement-rate tests.

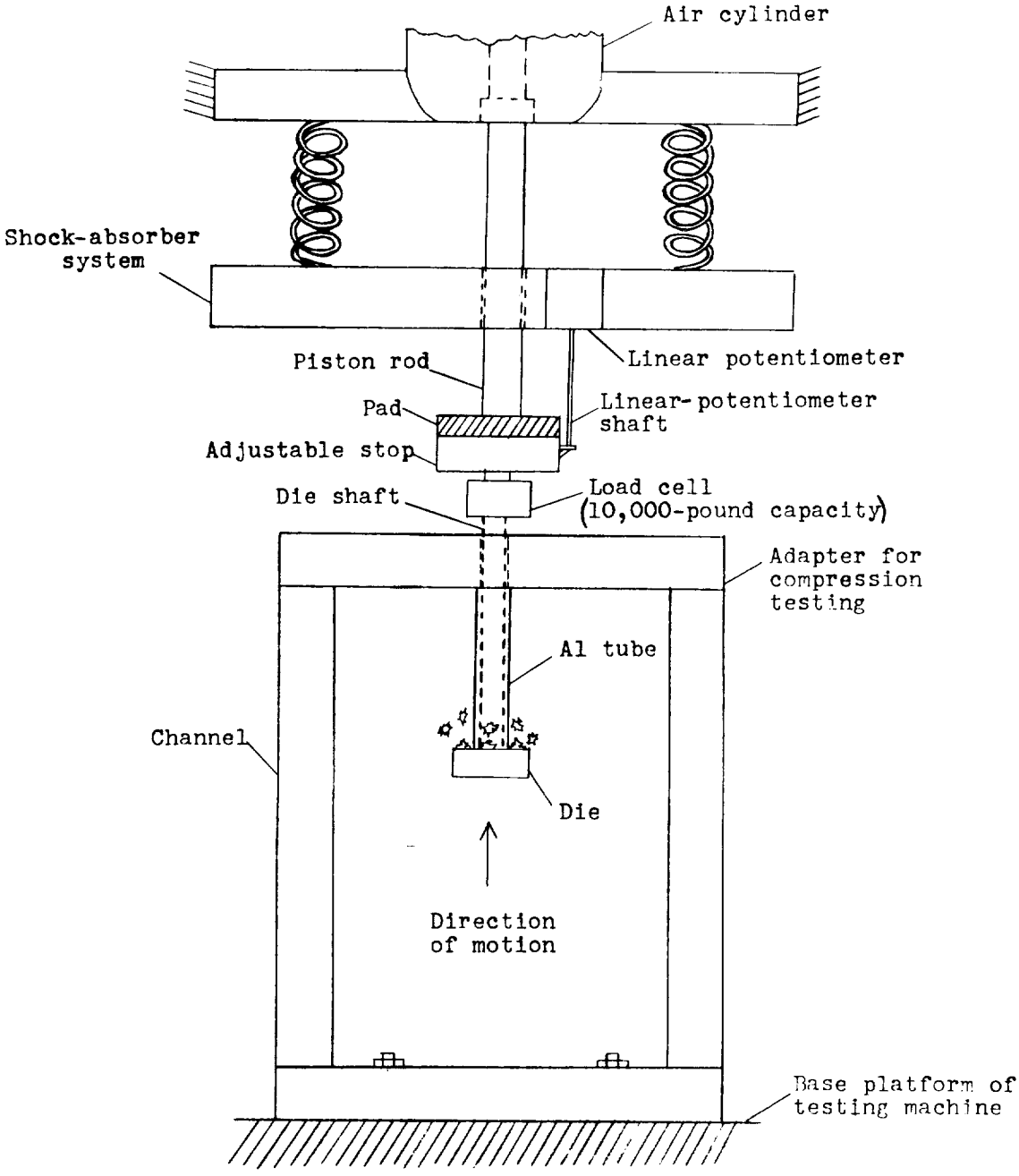


Figure 3.- Sketch of test setup in high-speed testing machine.

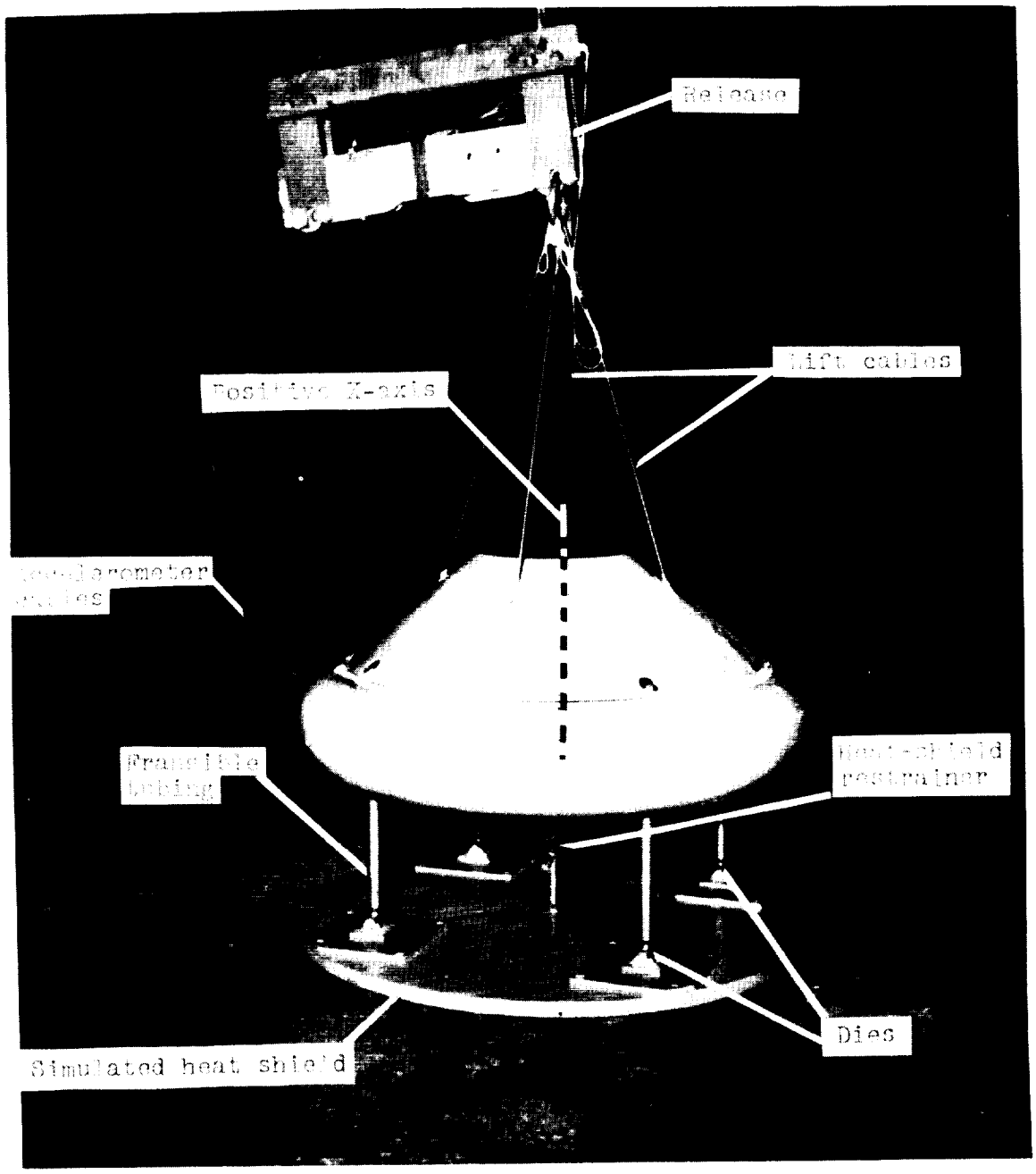


L-61-3479.1

Figure 4.- Photograph of 1/5-scale model used in landings from vertical flight path.

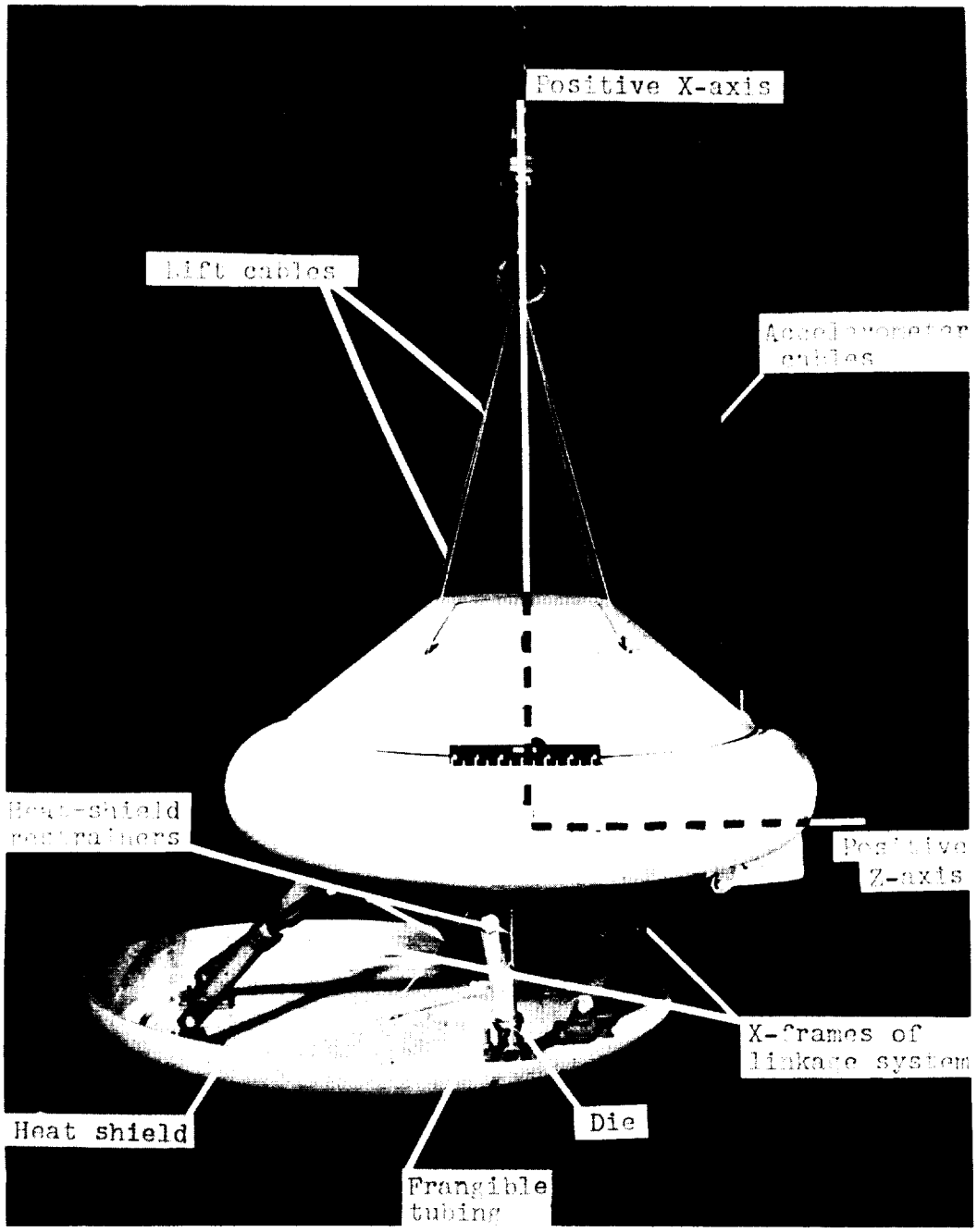


(a) Side view showing model axes. L-61-7603.1

Figure 5.- Photograph of 1/5-scale model used in landings from oblique flight path.

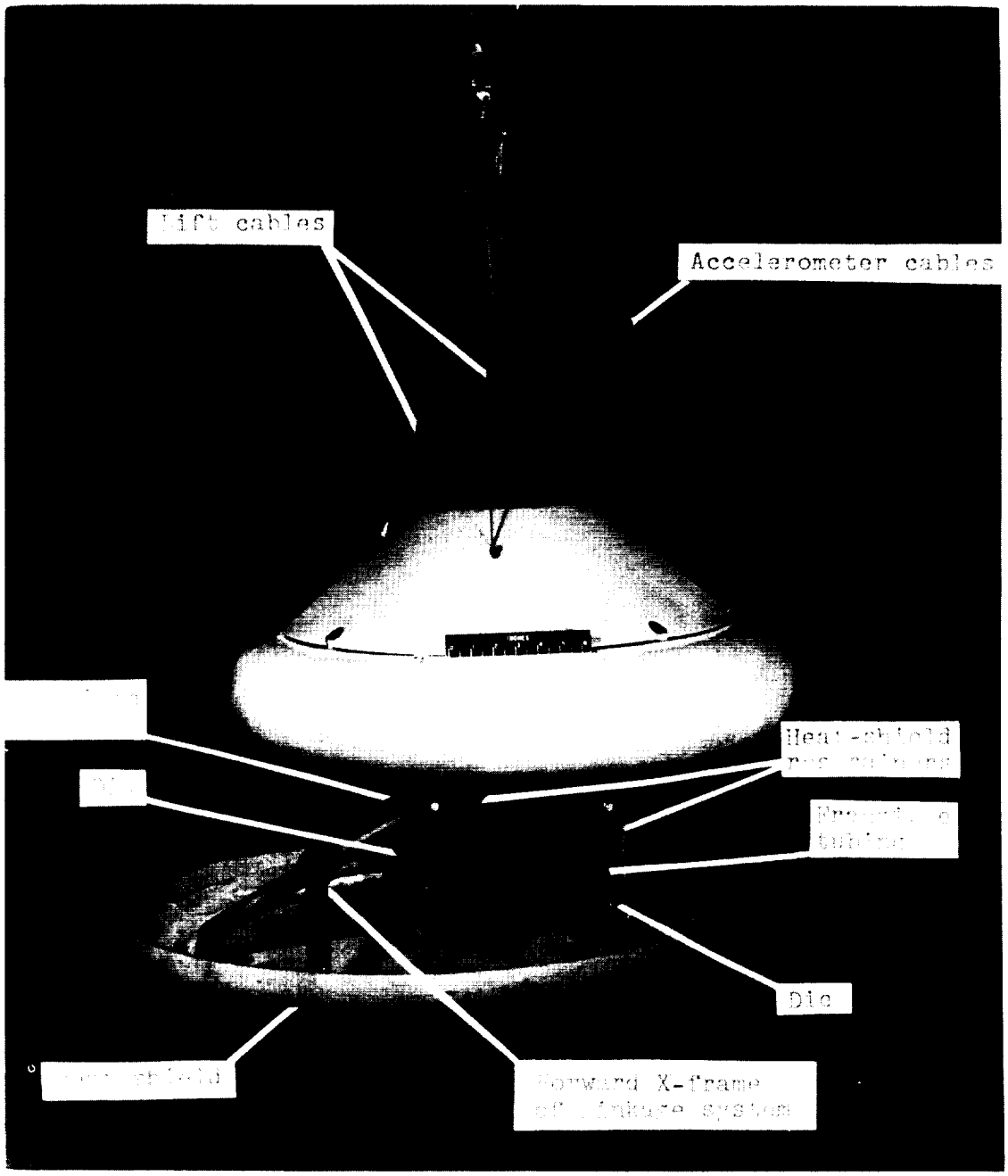


(b) Three-quarter front view. L-61-7601.1

Figure 5.- Concluded.

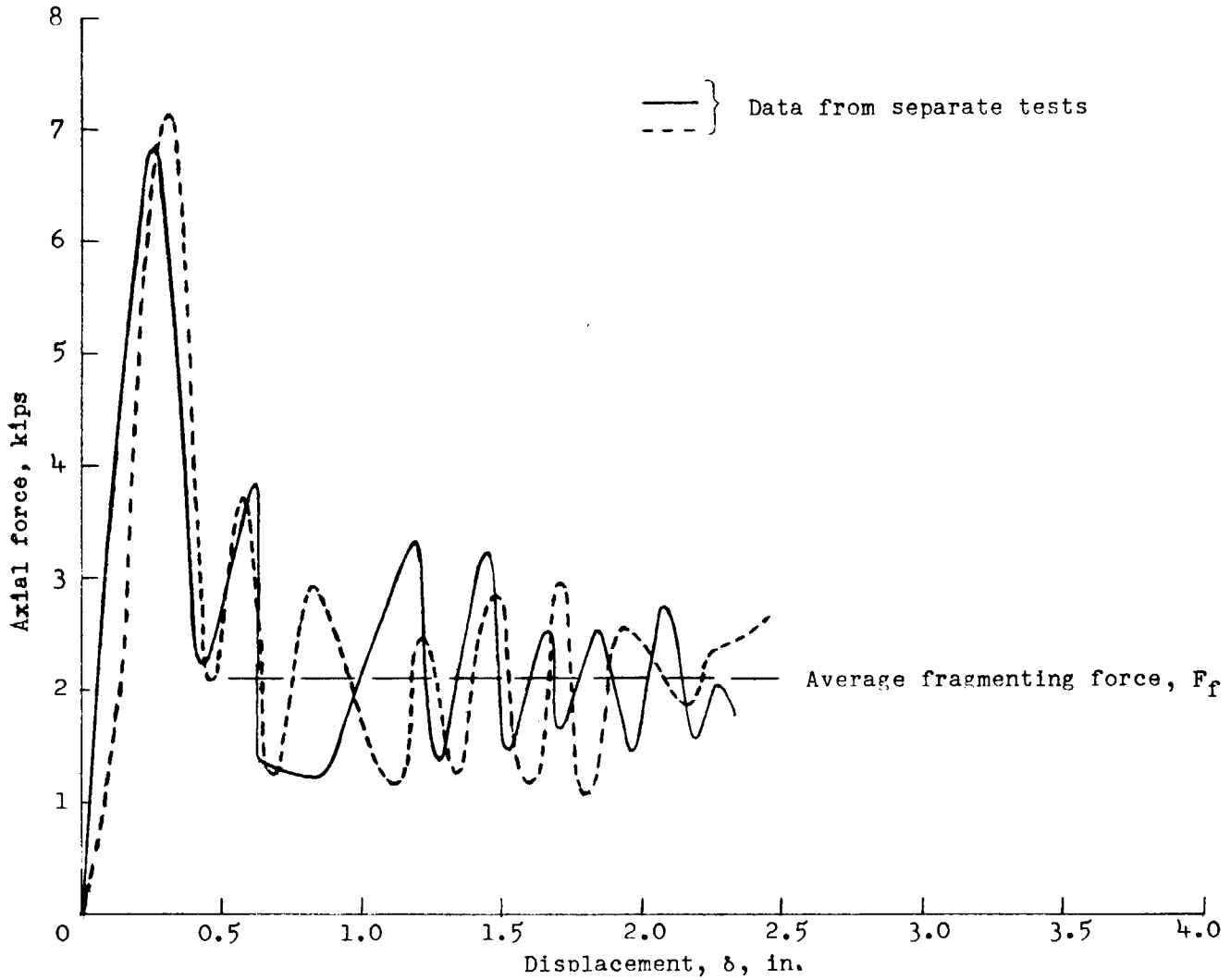


Figure 6.- Typical axial-force variations with displacement. 1-inch diameter; 0.065-inch wall thickness; t/r = 0.40; $\dot{\delta}$ = 1 inch per minute.

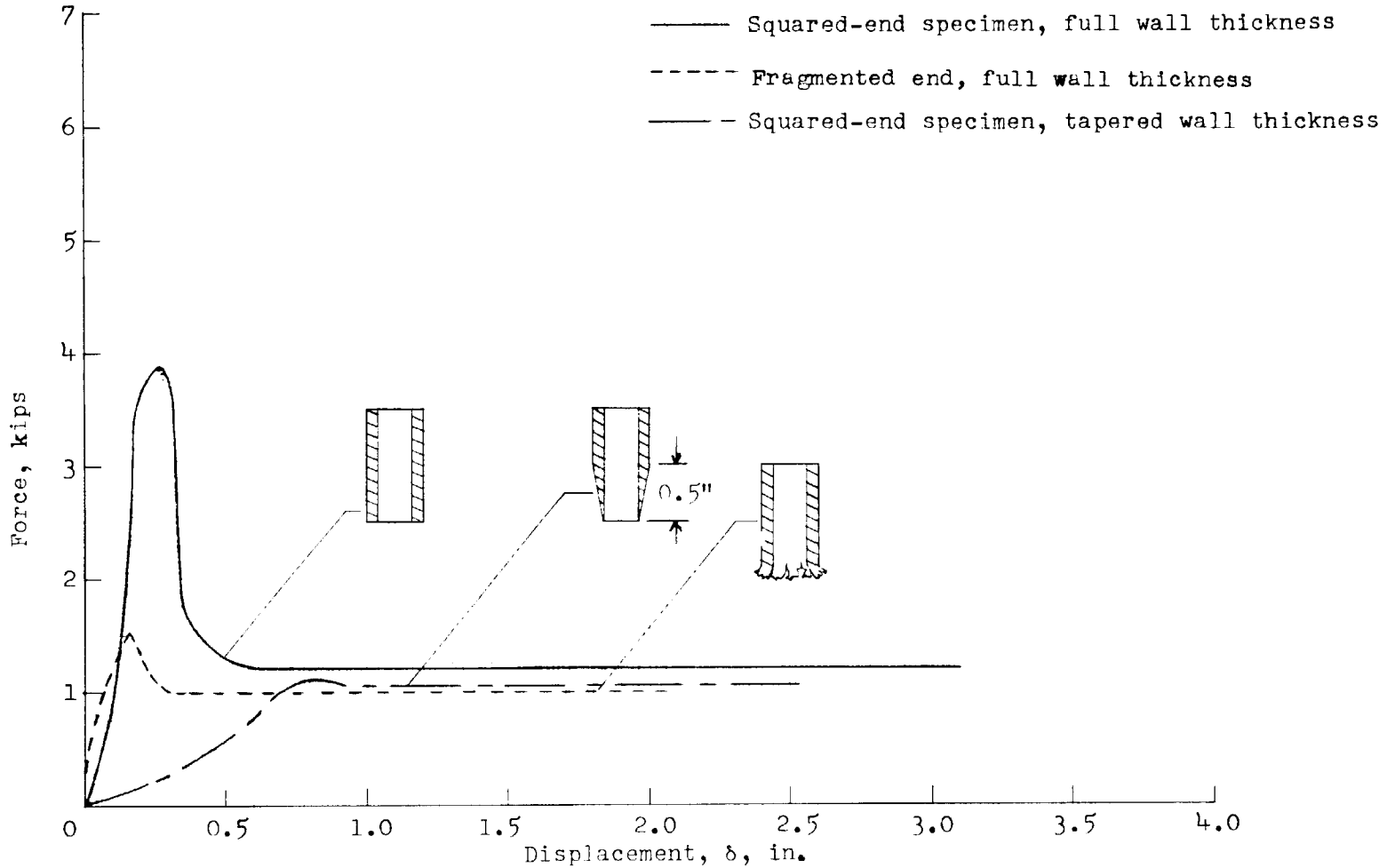


Figure 7.- Control of initial peak force. 0.5-inch diameter; 0.065-inch wall thickness; $t/r = 0.43$; $\dot{\delta} = 1$ inch per minute.

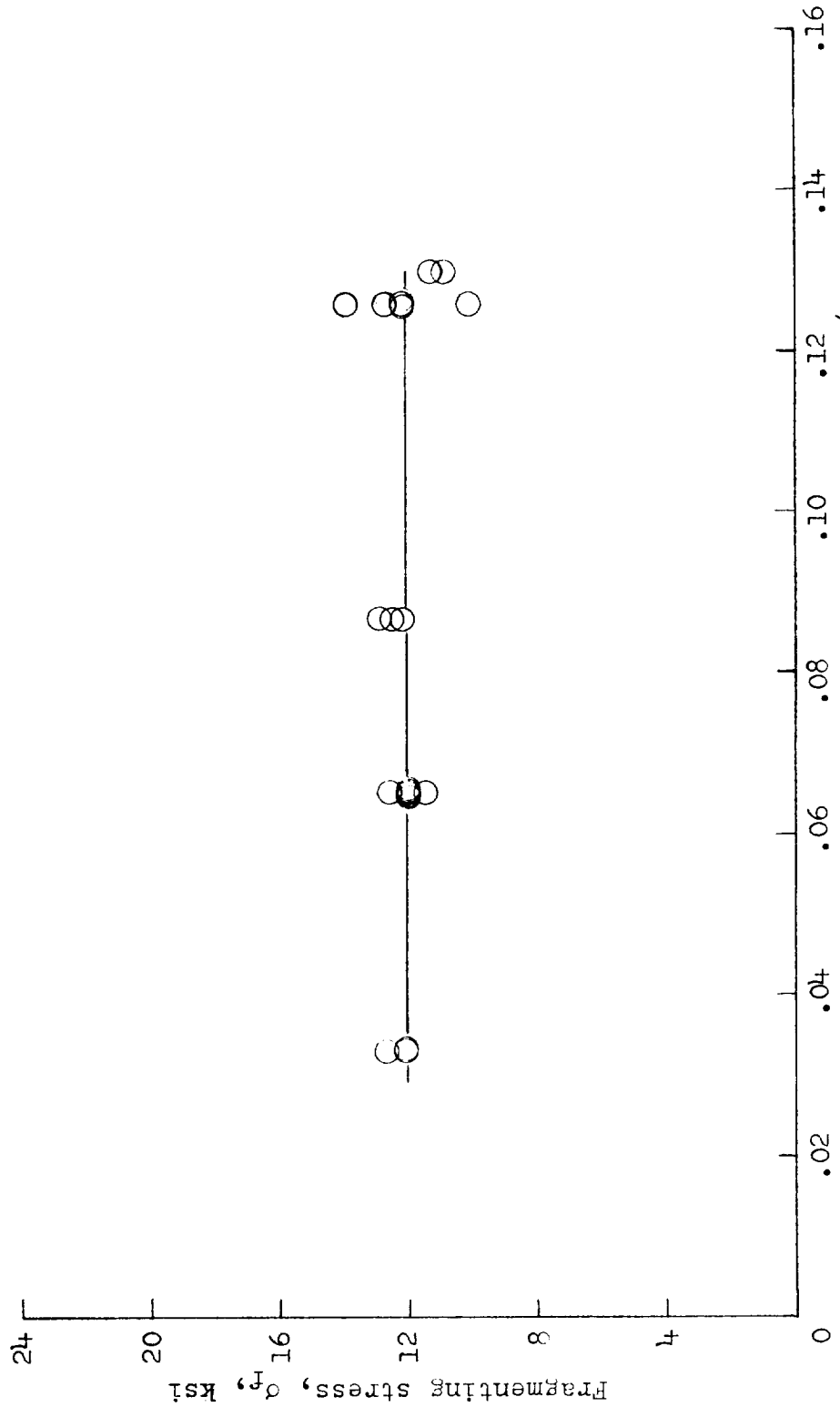


Figure 8.- Variation of fragmenting stress with tube wall thickness-diameter ratio. Wall thickness = 0.065 inch; $\dot{\delta}$ = 1 inch per minute; t/r = 0.43.

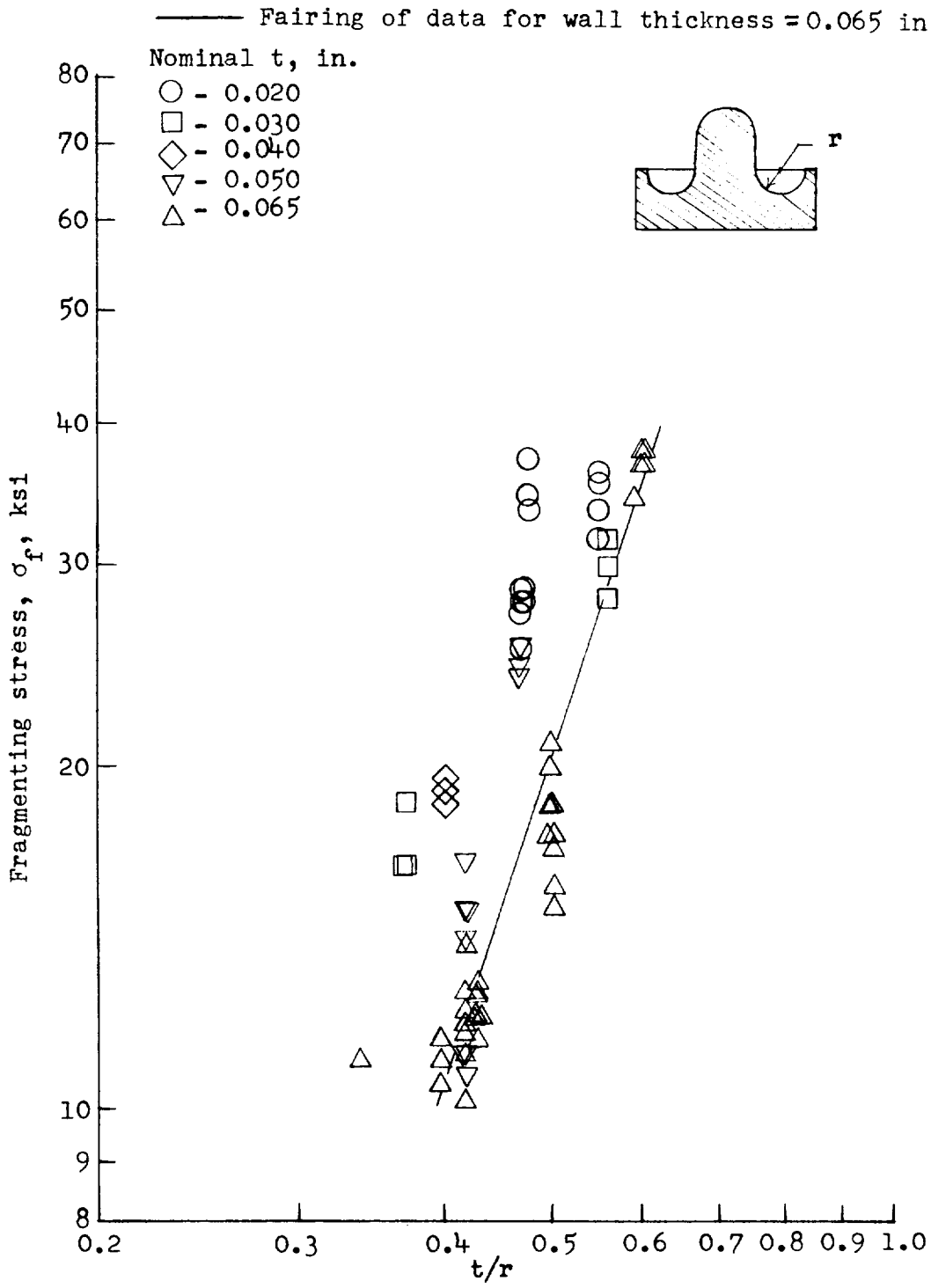


Figure 9.- Variation of fragmenting stress with t/r.

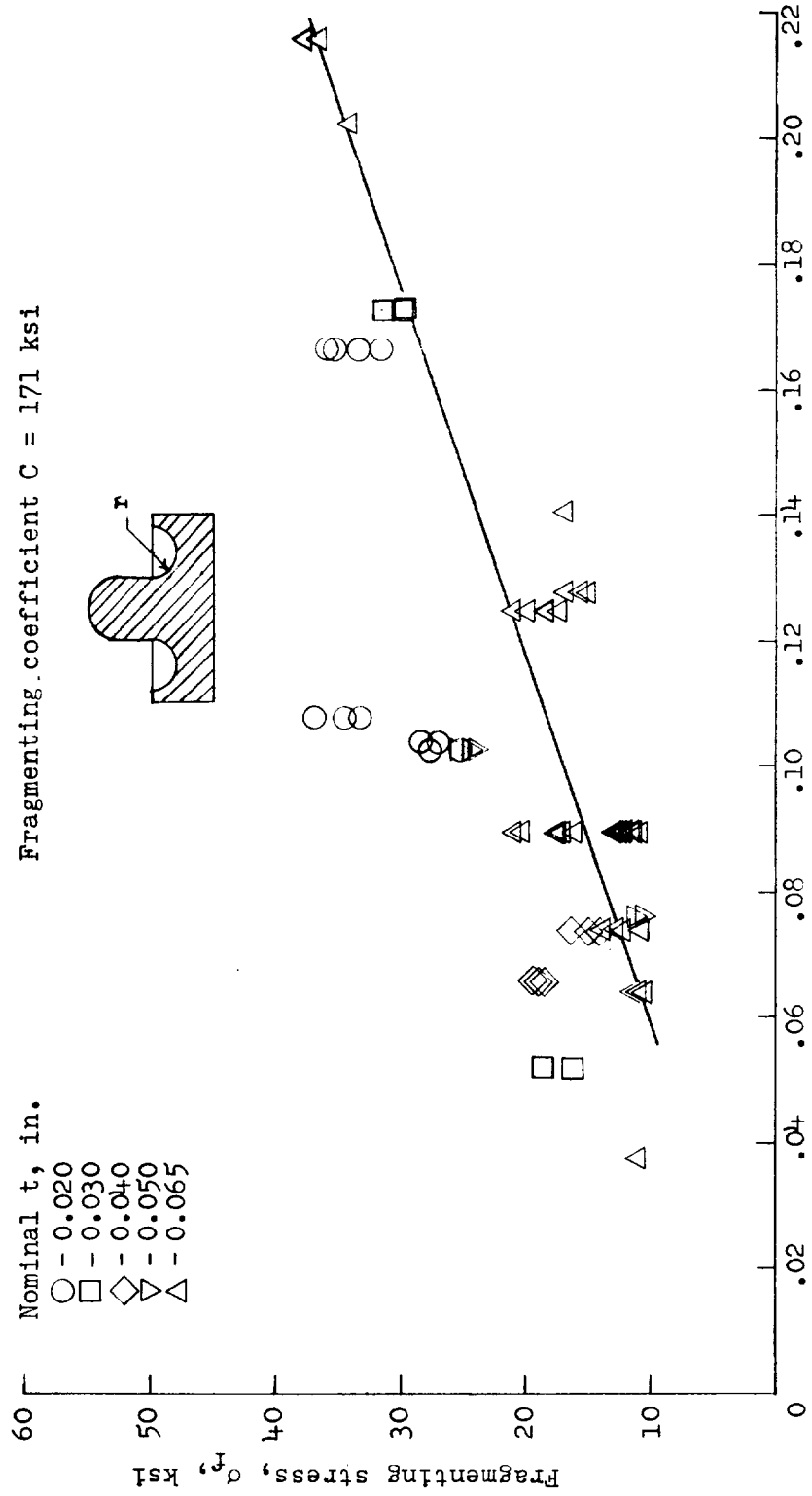


Figure 10.- Determination of fragmenting coefficient.

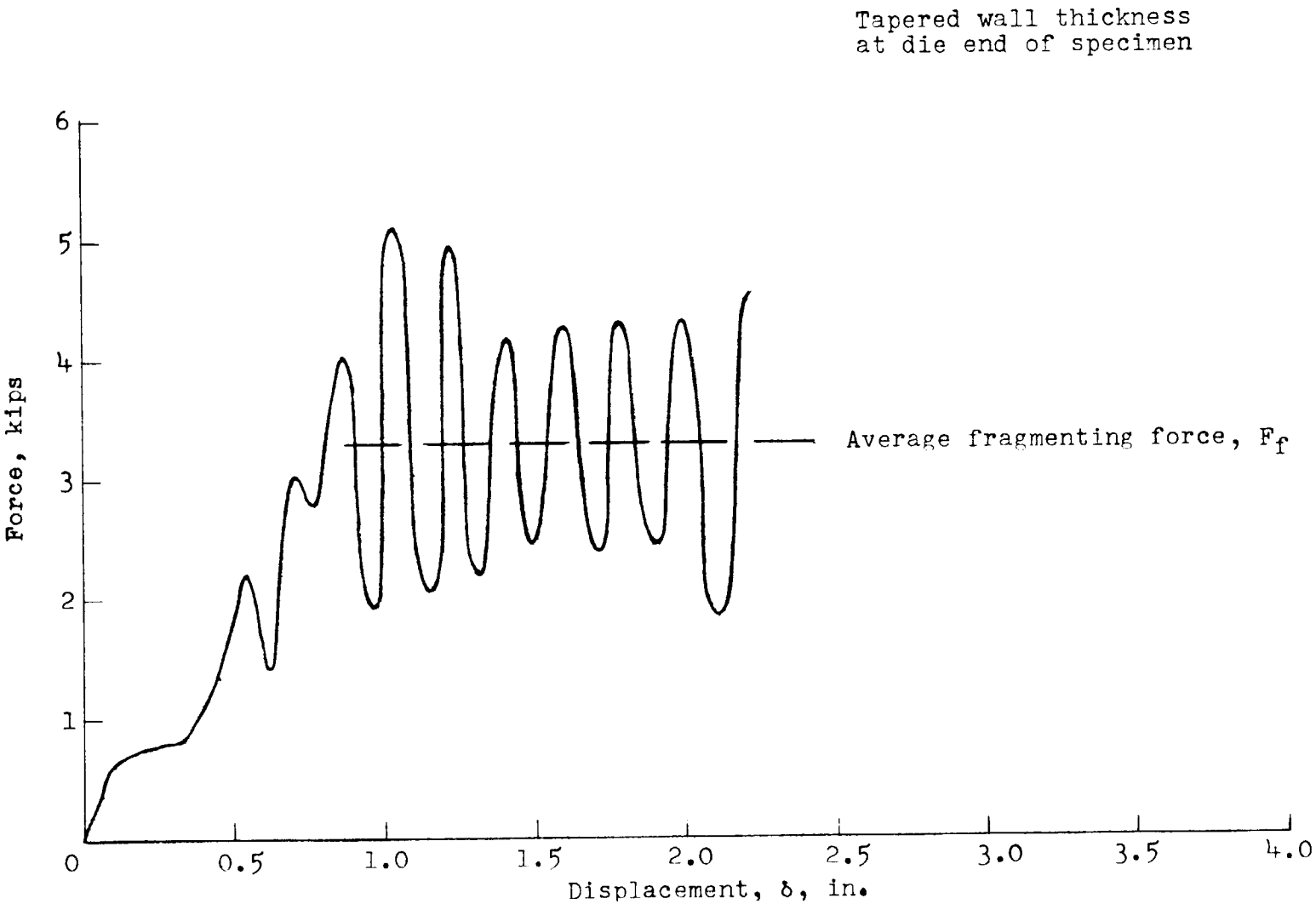


Figure 11.- Typical force variations with displacement. 1-inch diameter; 0.065-inch wall thickness; t/r = 0.43; $\dot{\delta}$ = 9,600 inches per minute.

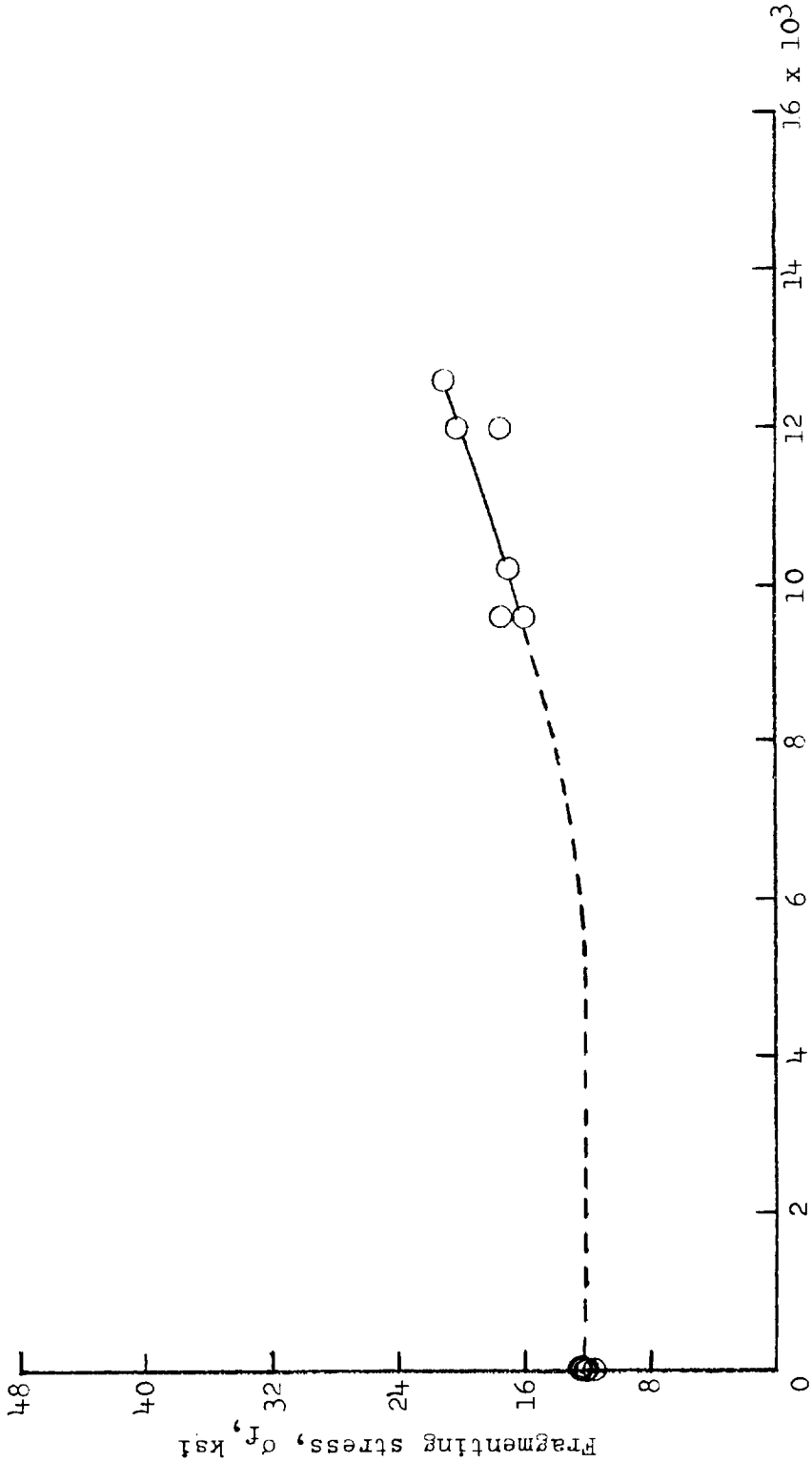


Figure 12.- Variation of fragmenting stress with rate of displacement. D = 1.0 inch; t = 0.065 inch; t/r = 0.43.

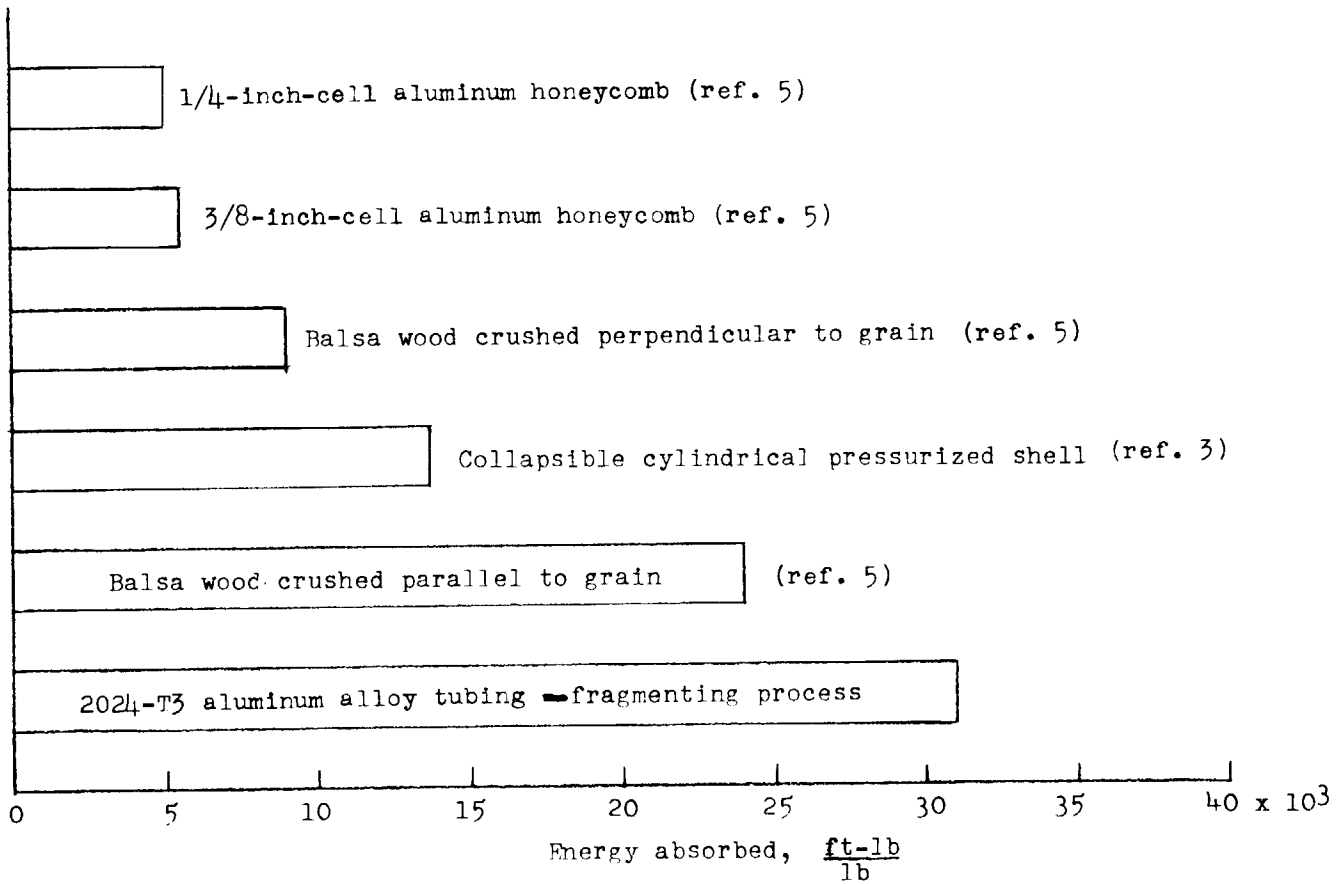


Figure 13.- Energy-absorption capabilities of various materials and processes.

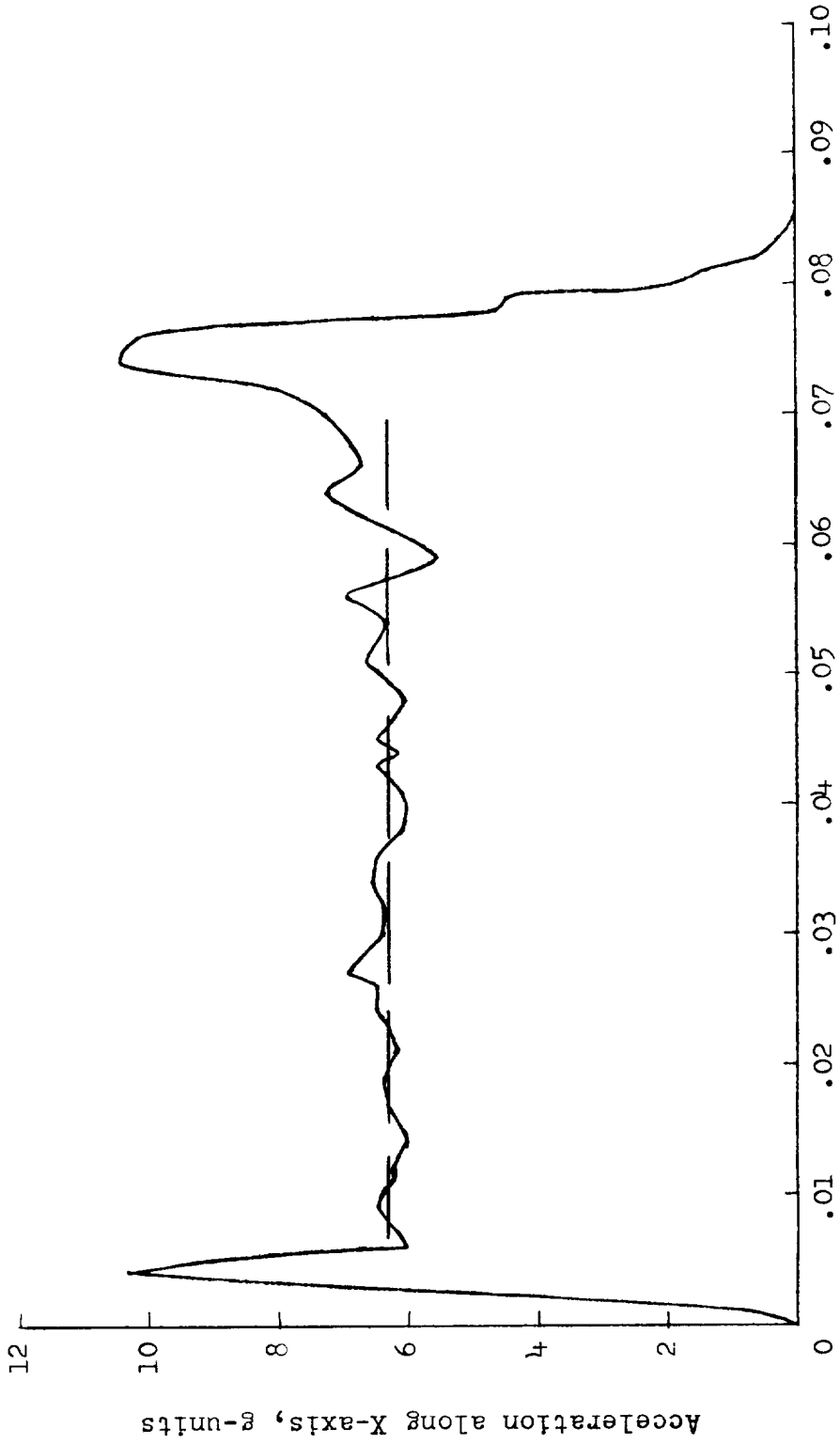


Figure 14.- Typical acceleration time history for model landing from 90° flight path onto concrete. Contact attitude, 0°; velocity at contact, 13.5 fps. All values are model scale.

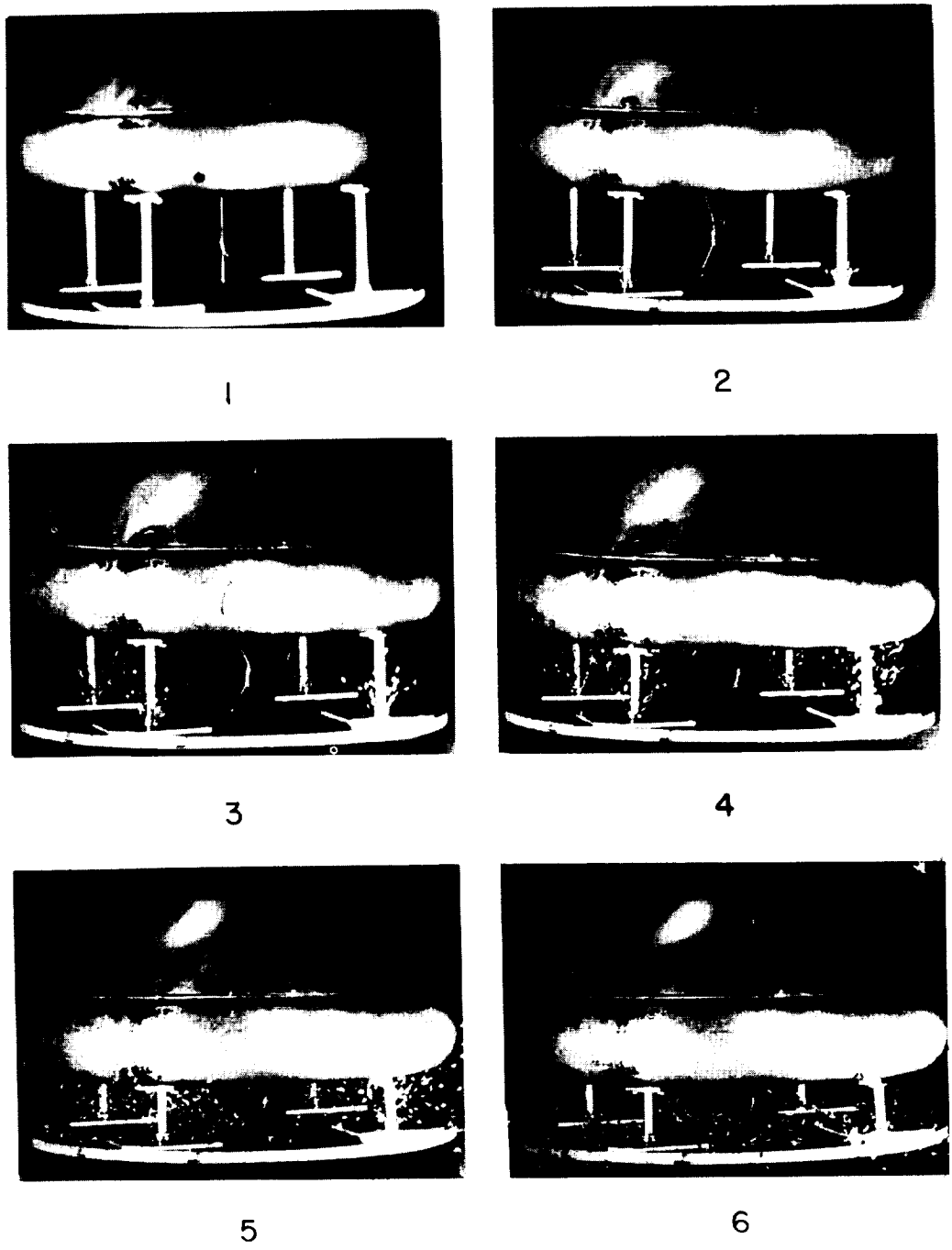


L-61-4808

Figure 15.- Sequence photographs of model landing from 90° flight path at a 0° contact attitude. Velocity at contact, 13.5 fps. All values are model scale.

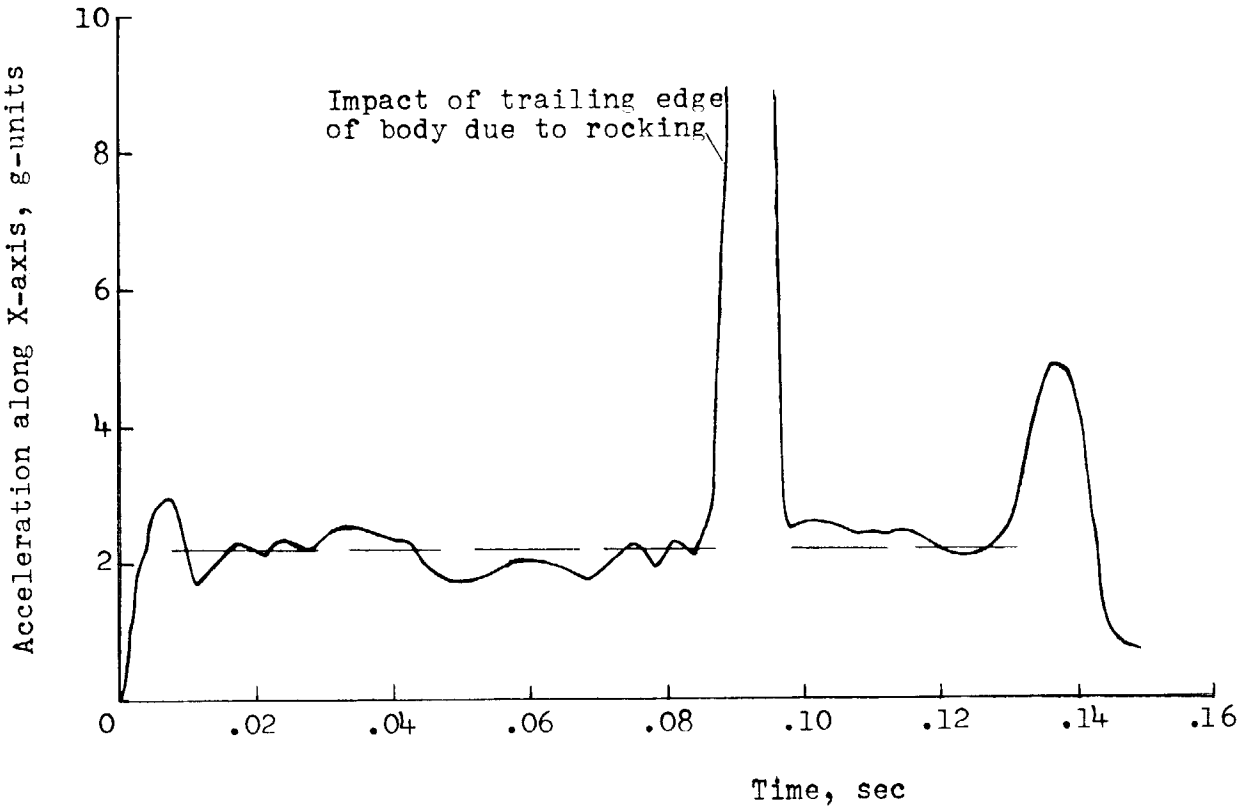


Figure 16.- Typical acceleration time history of model landing from 33° flight path onto concrete. Vertical velocity at contact, 4.7 fps; horizontal velocity at contact, 7.3 fps; contact attitude, 11°. All values are model scale.

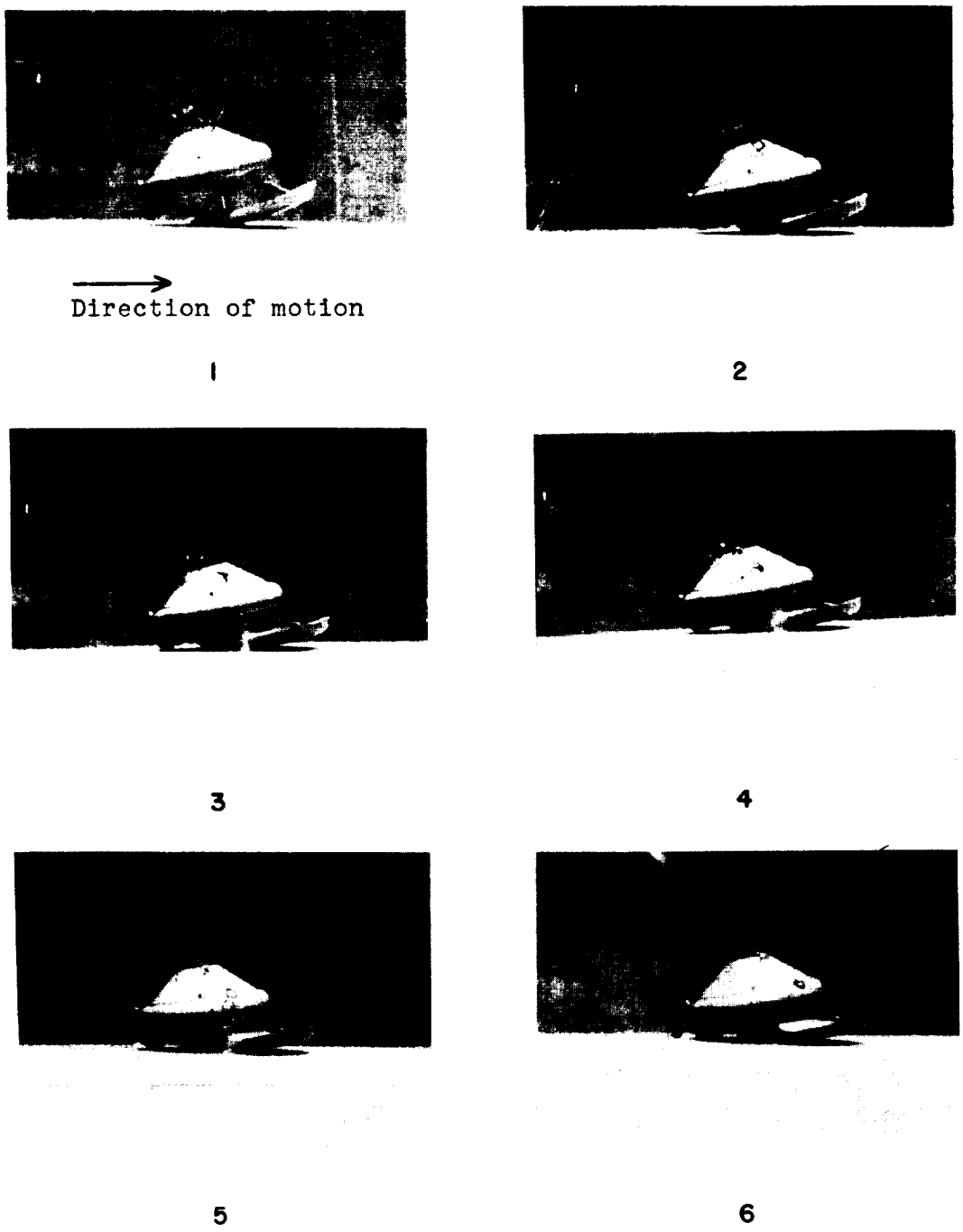


L-61-4813.1

Figure 17.- Sequence photographs of model landing from 36° flight path. Vertical velocity at contact, 6 fps; horizontal velocity at contact, 8 fps; contact attitude, 12°. All values are model scale.

NASA-Langley, 1962 L-2030

NASA TN D-1477
National Aeronautics and Space Administration.
A PRELIMINARY EXPERIMENTAL INVESTIGATION OF AN ENERGY-ABSORPTION PROCESS EMPLOYING FRANGIBLE METAL TUBING. John R. McGehee. October 1962. 34p. OTS price, $1.00. (NASA TECHNICAL NOTE D-1477)

A preliminary experimental investigation has been conducted to determine the variation of the average fragmenting stress with pertinent parameters and the feasibility of employing this process in a load-alleviation application. Model tests indicate that the process is suitable for use in a load-alleviation application.

I. McGehee, John R.
II. NASA TN D-1477

(Initial NASA distribution:
48, Space vehicles;
51, Stresses and loads;
52, Structures.)

NASA

NASA TN D-1477
National Aeronautics and Space Administration.
A PRELIMINARY EXPERIMENTAL INVESTIGATION OF AN ENERGY-ABSORPTION PROCESS EMPLOYING FRANGIBLE METAL TUBING. John R. McGehee. October 1962. 34p. OTS price, $1.00. (NASA TECHNICAL NOTE D-1477)

A preliminary experimental investigation has been conducted to determine the variation of the average fragmenting stress with pertinent parameters and the feasibility of employing this process in a load-alleviation application. Model tests indicate that the process is suitable for use in a load-alleviation application.

I. McGehee, John R.
II. NASA TN D-1477

(Initial NASA distribution:
48, Space vehicles;
51, Stresses and loads;
52, Structures.)

NASA

NASA TN D-1477
National Aeronautics and Space Administration.
A PRELIMINARY EXPERIMENTAL INVESTIGATION OF AN ENERGY-ABSORPTION PROCESS EMPLOYING FRANGIBLE METAL TUBING. John R. McGehee. October 1962. 34p. OTS price, $1.00. (NASA TECHNICAL NOTE D-1477)

A preliminary experimental investigation has been conducted to determine the variation of the average fragmenting stress with pertinent parameters and the feasibility of employing this process in a load-alleviation application. Model tests indicate that the process is suitable for use in a load-alleviation application.

I. McGehee, John R.
II. NASA TN D-1477

(Initial NASA distribution:
48, Space vehicles;
51, Stresses and loads;
52, Structures.)

NASA

NASA TN D-1477
National Aeronautics and Space Administration.
A PRELIMINARY EXPERIMENTAL INVESTIGATION OF AN ENERGY-ABSORPTION PROCESS EMPLOYING FRANGIBLE METAL TUBING. John R. McGehee. October 1962. 34p. OTS price, $1.00. (NASA TECHNICAL NOTE D-1477)

A preliminary experimental investigation has been conducted to determine the variation of the average fragmenting stress with pertinent parameters and the feasibility of employing this process in a load-alleviation application. Model tests indicate that the process is suitable for use in a load-alleviation application.

I. McGehee, John R.
II. NASA TN D-1477

(Initial NASA distribution:
48, Space vehicles;
51, Stresses and loads;
52, Structures.)

NASA

NASA TN D-1477
National Aeronautics and Space Administration.
A PRELIMINARY EXPERIMENTAL INVESTIGATION OF AN ENERGY-ABSORPTION PROCESS EMPLOYING FRANGIBLE METAL TUBING. John R. McGehee. October 1962. 34p. OTS price, $1.00. (NASA TECHNICAL NOTE D-1477)

A preliminary experimental investigation has been conducted to determine the variation of the average fragmenting stress with pertinent parameters and the feasibility of employing this process in a load-alleviation application. Model tests indicate that the process is suitable for use in a load-alleviation application.

I. McGehee, John R.
II. NASA TN D-1477

(Initial NASA distribution:
48, Space vehicles;
51, Stresses and loads;
52, Structures.)

NASA

NASA TN D-1477
National Aeronautics and Space Administration.
A PRELIMINARY EXPERIMENTAL INVESTIGATION OF AN ENERGY-ABSORPTION PROCESS EMPLOYING FRANGIBLE METAL TUBING. John R. McGehee. October 1962. 34p. OTS price, $1.00. (NASA TECHNICAL NOTE D-1477)

A preliminary experimental investigation has been conducted to determine the variation of the average fragmenting stress with pertinent parameters and the feasibility of employing this process in a load-alleviation application. Model tests indicate that the process is suitable for use in a load-alleviation application.

I. McGehee, John R.
II. NASA TN D-1477

(Initial NASA distribution:
48, Space vehicles;
51, Stresses and loads;
52, Structures.)

NASA

NASA TN D-1477
National Aeronautics and Space Administration.
A PRELIMINARY EXPERIMENTAL INVESTIGATION OF AN ENERGY-ABSORPTION PROCESS EMPLOYING FRANGIBLE METAL TUBING. John R. McGehee. October 1962. 34p. OTS price, $1.00. (NASA TECHNICAL NOTE D-1477)

A preliminary experimental investigation has been conducted to determine the variation of the average fragmenting stress with pertinent parameters and the feasibility of employing this process in a load-alleviation application. Model tests indicate that the process is suitable for use in a load-alleviation application.

I. McGehee, John R.
II. NASA TN D-1477

(Initial NASA distribution:
48, Space vehicles;
51, Stresses and loads;
52, Structures.)

NASA

NASA TN D-1477
National Aeronautics and Space Administration.
A PRELIMINARY EXPERIMENTAL INVESTIGATION OF AN ENERGY-ABSORPTION PROCESS EMPLOYING FRANGIBLE METAL TUBING. John R. McGehee. October 1962. 34p. OTS price, $1.00. (NASA TECHNICAL NOTE D-1477)

A preliminary experimental investigation has been conducted to determine the variation of the average fragmenting stress with pertinent parameters and the feasibility of employing this process in a load-alleviation application. Model tests indicate that the process is suitable for use in a load-alleviation application.

I. McGehee, John R.
II. NASA TN D-1477

(Initial NASA distribution:
48, Space vehicles;
51, Stresses and loads;
52, Structures.)

NASA